Transportation Research Part D 93 (2021) 102769

Contents lists available at ScienceDirect

Transportation Research Part D

journal homepage: www.elsevier.com/locate/trd

Electric vehicle fast charging infrastructure planning in urban networks considering daily travel and charging behavior

Mohammadreza Kavianipour [a], Fatemeh Fakhrmoosavi [a], Harprinderjot Singh [a], Mehrnaz Ghamami [a,*], Ali Zockaie [a], Yanfeng Ouyang [b], Robert Jackson [c]

[a] Michigan State University, 428 S. Shaw Lane, East Lansing, MI 48824, United States
[b] University of Illinois at Urbana-Champaign, 205 N. Mathews, 1209 Newmark Civil Engineering Bldg., Urbana, IL 61801, United States
[c] Michigan Department of Environment, Great Lakes, and Energy, 525 West Allegan Street, Lansing, MI 48909-7973, United States

ARTICLE INFO

Keywords:
Charging station planning
Electric vehicles
Fast charging
Urban network
Detour
Queue
System optimization

ABSTRACT

Electric vehicles are a sustainable substitution to conventional vehicles. This study introduces an integrated framework for urban fast charging infrastructure to address the range anxiety issue. A mesoscopic simulation tool is developed to generate trip trajectories, and simulate charging behavior based on various trip attributes. The resulting charging demand is the key input to a mixed-integer nonlinear program that seeks charging station configuration. The model minimizes the total system cost including charging station and charger installation costs, and charging, queuing, and detouring delays. The problem is solved using a decomposition technique incorporating a commercial solver for small networks, and a heuristic algorithm for large-scale networks, in addition to the Golden Section method. The solution quality and significant superiority in the computational efficiency of the decomposition approach are confirmed in comparison with the implicit enumeration approach. Furthermore, the required infrastructure to support urban trips is explored for future market shares and technologies.

1. Introduction

Crude oil price fluctuations and major concerns about vehicle emissions have pushed the car industry towards investment in electric vehicle (EV) production (Dong et al., 2014; He et al., 2013; Kavianipour et al., 2020). EVs remove on-road emissions and can mitigate air pollution significantly if accompanied by green energy production. Limited driving range and insufficient supporting infrastructure, as well as long charging times, however, have hindered the acceptance of the EVs in the market (He et al., 2013; Nie and Ghamami, 2013). Although some current EV models can exceed 300 miles per charge, the range is still lower than that of similar conventional vehicles (CV). Also, unlike CVs, the performance of EVs decreases further in cold weather (Krisher, 2019). Therefore, customers are concerned about being stranded along their way by running out of charge while without access to charging stations, called range anxiety (Tate et al., 2008). Providing adequate charging infrastructure mitigates some such challenges associated with EVs, and is known to be among the main factors to increase their market share (Nie et al., 2016).

The driving pattern of EVs with their initial state of charge can be used to determine the optimal location of charging stations. Some

* Corresponding author.
E-mail addresses: kavianip@egr.msu.edu (M. Kavianipour), moosavi@egr.msu.edu (F. Fakhrmoosavi), singhh24@msu.edu (H. Singh), ghamamim@egr.msu.edu (M. Ghamami), zockaiea@egr.msu.edu (A. Zockaie), yfouyang@illinois.edu (Y. Ouyang), JacksonR20@michigan.gov (R. Jackson).

https://doi.org/10.1016/j.trd.2021.102769

Available online 2 March 2021

studies have used travel surveys, e.g. National Household Travel Survey and Metropolitan Travel Survey Archive, to find the users' driving pattern information including trip travel times, distances, origins, and destinations (Andrews et al., 2012; Avci et al., 2012; Sweda and Klabjan, 2011). Taxi GPS data can also provide similar information, but their applications are limited to charging station planning for on-demand ride services (Shahraki et al., 2015; Tu et al., 2016). Due to the unavailability of EV trajectories, simulation-based data sets can be used as a surrogate (Dong et al., 2014; Xi et al., 2013).

The main focus of this study is on developing an integrated modeling framework for urban charging infrastructure planning, considering DC fast chargers with 50–150 kW charging powers. Distances of single urban trips are generally much shorter than the range of typical EVs in the market, but vehicles are supposed to serve a daily chain of trips instead of a single trip. Also, not all urban trips can begin with fully charged batteries due to various reasons such as unavailability of level 2 (L2, with 6.2 kW power) chargers (Wood et al., 2017), lack of charging time, or owners simply forgetting to fully recharge overnight. This calls for a comprehensive data set that includes daily chains of trips for all travelers and availability of level 2 chargers at each intermediate destination. However, most of the urban planning agencies do not have access to these data, and rely on static zone-to-zone demand tables with aggregate data on trip purposes and land use characteristics at zone levels. Thus, an innovative approach is developed in this study to: (i) generate required dynamic travel demand information from available aggregate data, (ii) build a charging behavior simulation tool to assign the stochastic initial state of charge for each vehicle trajectory according to the departure time, trip purpose, and land use characteristics at the origin, (iii) feed this spatial and temporal distribution of charging demand into a micro-simulation charging infrastructure optimization framework, which captures travelers' charging behavior for a given market share of EVs, and ensures the feasibility of all EV trips. The mathematical model is decomposed into two subproblems that find the optimal location of stations and the number of chargers at each location separately.

The state-wide roadway network in Michigan provided by the Michigan Department of Transportation (MDOT) is considered as the main network of interest. Real-time traffic volume observations from loop detectors are used together with daily static demand data to estimate time-dependent demand tables. Then, a simulation-based dynamic traffic assignment tool, DYNASMART-P (Jayakrishnan et al., 1994), is used to provide trip trajectories, and zone-to-zone time-dependent travel time and distance skims. Time-dependent trip purposes are also available from a travel survey in Michigan (Wilaby and Casas, 2016). Finally, land-use attributes at origin and destination zones are used to determine trip purposes and to simulate charging behavior for any city of interest in the state-wide network. Regional networks for three cities with various sizes, namely Marquette, Lansing, and Detroit, are used to demonstrate the successful implementation of the proposed optimization framework for various charging technological advancement.

The remainder of this paper is organized as follows. The next section provides a literature review on charging station optimization and lists the key contributions of this study. The research framework section then presents the traffic simulation model, the charging behavior simulation model, and optimization model, as well as a solution methodology. Next there are demonstrations of numerical experiments including setup of the case studies, data, and results. The final section provides concluding remarks and future research directions.

2. Literature review

To address the concerns on EVs, many studies have investigated the charging station location problem. The main steps in planning charging stations are finding the charging demand and providing chargers at stations to serve this demand. Two common approaches are exploited to locate stations. The first approach clusters the charging demand and deploys stations to meet this demand (Ip et al., 2010). The other approach considers the demand as network flow (Hodgson, 1990) and maximizes the captured flow by providing the charging stations on the intersecting roads. Other variants of this model consider the charging behavior of vehicles to find the locations that maximize the number of served vehicles (Kim and Kuby, 2012; Kuby and Lim, 2005; Upchurch et al., 2009). Even though the models considering demand as flow or clusters at nodes of the network are well-suited to capture the intercity trips of EV users, they might not serve the urban trips of EV users the best because they include a combination of trips. This study presents a framework simulating EV charging behavior and charging demand in urban areas using trip-based demand models. The current models are also applied to intercity networks where users start their trips with a similar state of charge. However, EVs begin their urban trips with different states of charge, which mandates considering the charging demand in more detail. One of the main contributions of this study is capturing variations in charging demand based on trips and land use characteristics. To find the charging demand in urban networks, one approach is to incorporate data-driven models developed from travel surveys considering endpoint, distance, purpose, departure time, and arrival time of each trip. The charging demand is then used to select charging stations from a set of candidate locations to minimize the number of unfulfilled trips (Andrews et al., 2012; Chen et al., 2013). Another approach is to incorporate a micro-simulation approach developed based on travel surveys to simulate all trips and have an extensive dataset, including the trajectory of vehicles. This approach provides the opportunity to solve complex problems under various hypothetical scenarios that often cannot be addressed directly from survey data (e.g., due to small sample sizes). In this study, we propose to use this approach to simulate vehicle trajectories and have access to information such as departure time and the initial state of charge, to capture the temporal variations in travel times and shortest paths. These features are necessary to be considered for planning and designing infrastructure in urban networks (specially for charging stations of EVs), which the proposed micro-simulation model in this study considers.

Beside using travel survey data, exploiting trip trajectory travel data is another common approach to find the charging demand. The trip trajectory of taxis has been used in numerous studies; e.g., to identify the locations with longest dwell times as the candidate points (Cai et al., 2014), adopt an optimization-based approach to find the hotspots maximizing the vehicles-miles-traveled (VMT) on electricity (Shahraki et al., 2015), and minimize the infrastructure cost considering congestion at charging stations (Yang et al., 2017). The models using taxi trajectories can be applied for taxis or buses, but are not suitable for private EVs due to the limited availability of

GPS data. Therefore, an alternative approach to capture travel data is to use traffic simulation for the origin-destination demand tables. In this regard, some studies consider the fixed-route choice and travel patterns (Berman et al., 1992; Hodgson, 1990; Kuby and Lim, 2007, 2005; Lim and Kuby, 2010; Nourbakhsh and Ouyang, 2010; Upchurch et al., 2009; Xie et al., 2016; Zockaie et al., 2016), while others capture the interactions between service facility locations and the traffic assignment problem (Bai et al., 2011; Fakhrmoosavi et al., 2021; Ghamami et al., 2020; Hajibabai et al., 2014; He et al., 2013, 2018; Kavianipour et al., 2021; Riemann et al., 2015). Capturing these interactions makes the problem computationally cumbersome in large scale networks. This study relies on traffic simulation to generate vehicle trajectories. It captures the interaction between charging station locations and assignment of vehicles, then introduces a heuristic technique to reduce the problem.

Due to the lack of real-world data on details of EVs' trip trajectories, and their state of charge along their trips, simulation tools were implemented to generate this data. Some studies locate charging stations using a simulation-optimization model, minimizing investment cost for different types of chargers and/or the number of trajectories that are unable to reach their destination due to the lack of infrastructure (Dong et al., 2014; Xi et al., 2013). Another approach adopts real-time trajectories of taxis, and uses a time-series simulation model for traveling and charging behavior of plug-in hybrid electric vehicles, so as to provide insights on optimal charging station development plans (Li et al., 2017). This study addresses unavailability of charging and trip trajectory data by developing a state-of-charge simulator within a simulation-optimization framework.

The queuing delay is usually incorporated into a bi-level or single-level problem to determine the number of chargers. Xie et al. (2018) defined one feasible path for each OD pair and provided enough chargers to certify a certain level of service under stochastic queuing. A stochastic queuing model is adopted in Yang et al. (2017) as well, and the nonlinear queuing constraints in the optimization models are linearized with logarithmic transformation, and the models solved using commercial solvers. Some studies also consider the impact of queuing on the assignment of users. Jung et al. (2014) located the charging stations for electric taxis via a stochastic dynamic itinerary-interception model with stochastic queuing delay. They considered that users have information on the expected queuing delay in each charging station, which affects their assignments decisions through a bi-level setting. The lower level incorporates an activity-based simulation framework to capture the routing behavior of EVs based on the charging stations and chargers found in the upper level. Another study defined different charging scenarios and embedded the expected waiting time under stochastic queuing into link travel times, assuming that EVs have access to the expected waiting time information (Wang et al., 2019). Ghamami et al. (2020) developed a bi-level model to investigate the optimum charging infrastructure considering deterministic queuing in intercity networks. The user equilibrium at the lower level assumes that users have information on queuing delay and charging station availability (Ghamami et al., 2020). Similarly, Chen et al. (2020) found the optimum charging infrastructure through a bi-level problem where stochastic queuing was incorporated at the lower level, while Zhang et al. (2018) investigated joint operations and pricing mechanisms of coupled power and electric transportation systems for electric unmanned aerial vehicles. In this study, we assume queuing delay information is available through different platforms (i.e., charging station apps), and users are assigned based on the availability of charging stations and chargers. Our modeling framework considers either deterministic or stochastic queuing delay at charging stations. When the arrival rate exceeds the service rate, random fluctuations in the arrival and service processes will tend to cancel out, and hence we use deterministic queueing, which simply assumes uniform arrival and services. When the service rate is greater than the arrival rate, however, the deterministic queuing delay would be zero, which fails to capture the random surges in arrivals or services. In such a case, the stochastic queuing delay model would be considered, assuming a Poisson distribution for the arrival of vehicles and exponential distribution for service times. Either way, the charging station power capacity and the number of chargers (decision variables) determine the service rate, and the assignment of users to each charging station (state variables) determines the arrival rate.

To the best of the authors' knowledge, there is no study which considers all the components we include in this study. We reviewed the exact impact of queuing on the assignment of users, while other studies just consider the average queuing. Further, the problem formulation is comprehensive, reviewing every constraint required for the assignment of vehicles. Compared to the previous studies in charging station planning, this study contributes to the literature in the following aspects: 1) Presenting a framework simulating EV charging behavior and charging demand in urban areas using trip-based demand models; 2) Considering the initial state of charge variations, range anxiety, detour delay, charging delay, and queuing delay for each user; 3) Using a decomposition technique to

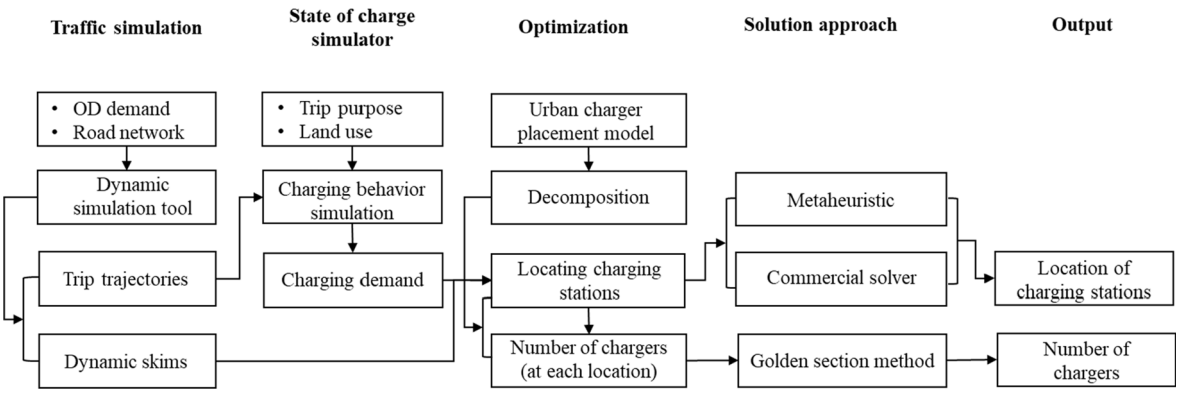

Fig. 1. Components in the proposed research framework.

effectively solve the problem; 4) Developing a framework that distinguishes between deterministic and stochastic queueing delays based on relative arrival and service rates; 5) Incorporating calibrated and realistic input parameters based on various stakeholders' feedback from real-world case studies to provide meaningful insights for system planners.

3. Research framework

This section first presents the proposed research framework (Fig. 1) by demonstrating the connections between traffic simulation, charging behavior simulation, and a mathematical optimization model. The traffic simulation component uses the Origin-Destination (OD) demand table and road network properties as inputs, incorporating a simulation-based dynamic traffic assignment tool (DYNASMART-P), to analyze the travelers' route choice behavior. Trip trajectories and skim tables are the main output of this component. The former includes traveled paths and travel time stamps along each path for each vehicle, and the latter are the average zone-to-zone travel distances and times. The next component, charging behavior simulation, utilizes temporal distribution of trip purposes, land use data, and trip trajectories from the first component to simulate travelers' charging behavior based on a random distribution of the initial state of charge and the required energy to complete their trips. The vehicles unable to fulfill their trips need to be recharged, forming the charging demand. This charging demand along with travel skims will be fed into an micro-simulation based urban charging infrastructure planning model. This model, which is formulated as a nonlinear mixed-integer program, is decomposed into two subproblems; one locates the charging stations in the network, and the other finds the number of chargers at each station.

This section also presents a decomposition approach to solve the mathematical optimization model. The problem is decomposed into two subproblems; one locates the charging stations in the network, and the other finds the number of chargers at each station. First, the cost function of the first subproblem, which includes charging stations' costs and users' refueling times and travel detours, is minimized to determine the locations for charging station installation. In this cost function, refueling times and detour times are monetized by incorporating the average value of time. Please note that this subproblem minimizes the energy required for the EVs to reach the charging stations, since the detour and refueling times are functions of energy consumption. This subproblem also ensures that all EVs can fulfill their trips by visiting one of the built charging stations. The solution of the first subproblem provides the time-dependent incoming traffic flow and energy demand in each station. This information is then used in the second subproblem to find the number of chargers needed to minimize the charger installation cost and users' waiting time cost (deterministic or stochastic). In fact, this subproblem minimizes the time loss under the condition provided by the first subproblem, i.e., minimal energy. The first subproblem is a linear mixed-integer mathematical model. While commercial solvers, e.g. CPLEX and Gurobi, can solve it for small-scale networks, a metaheuristic algorithm is developed in this study for larger-scale networks in this study. The second subproblem is a nonlinear mixed-integer mathematical model whose objective function is proven to be convex in Appendix B, and hence, the golden section method is proposed to solve this subproblem.

3.1. Traffic and charging behavior simulation

The statewide road network of Michigan consists of 37,125 links, 16,976 nodes, and 2,330 traffic analysis zones. The static demand matrix for different OD pairs is provided on a daily basis by the Michigan Department of Transportation (MDOT). Hourly factors are multiplied into the static demands to convert them into a time-dependent OD demand matrix. Hourly factors are estimated based on the information of 122 loop detectors installed across Michigan highways. These loop detectors are mostly located inside the city boundaries, which are the focus of the current study. For example, Detroit, Lansing, and Marquette networks contain 46, 20, and 2 loop detectors on their links, respectively. To consider the directionality of traffic during different hours of a day, the closest loop detector counting the traffic of the same direction as the OD pair direction is found. Based on the traffic counts of the selected loop detector for the OD pair of interest, the hourly demand factors are then defined for the OD pair.

Travelers' route choice is a collective decision-making process that results in a certain traffic state and congestion level at the network level. Traffic simulation provides trip trajectories that can be used to predict the time-dependent charging demand. Each trajectory provides information regarding the chosen path, timestamps of travel along the path, origin zone, destination zone, departure time interval, vehicle type (randomly assigned, based on the given market share), total travel time, and total travel distance. In this study, a mesoscopic traffic simulation tool, DYNASMART-P, is incorporated to provide user information applicable to the statewide network of Michigan, and then the required trip trajectories for the cities of interest are extracted. The trajectories of all vehicles, along with the dynamic skims including travel times and distances for every OD-pair, are reported as the outputs of this research component.

Intercity trips are often considered as stand-alone trips, in which EVs are highly likely to have fully charged batteries due to their preplanned nature. Urban trips, however, are part of a chain of trips, in which EVs might have any state of charge (depending on the availability of chargers and dwell time for recharging at the trip origin). Therefore, the charging incidence in one trip may depend on its sequential trip as well, i.e., the vehicle might recharge during a feasible trip to prevent charging in a subsequent infeasible one (Usman et al., 2020). However, the availability of trip chain information is still limited and transportation agencies still rely on zone-to-zone OD demand tables. Therefore, developing a framework to capture the EVs charging demand based on zone-to-zone OD demands is crucial. In this study, a simulation tool is developed to estimate the charging behavior of EVs based on their departure time, trip purpose, and land use characteristics of their origin and destination zones. The simulation tool estimates the initial state of charge at the origin, and the desired state of charge that the EV drivers prefer to have upon arrival at the destination.

The proposed simulation tool assumes that users departing from home/workplace have a higher chance to have access to level 2 chargers than those departing from other areas. While home charging is the dominant way to charge EVs, some workplaces provide

level 2 charging facilities for their employees. Therefore, the proposed simulation tool distinguishes the trips that begin from home/workplace by assigning them a higher initial state of charge. Further, it considers a higher initial state of charge for single-family residential areas than multi-family ones because the former have more space/authority to deploy chargers. The simulation tool incorporates a survey conducted by MDOT in 2016 (Wilaby and Casas, 2016) that presents the time-dependent trip purpose distribution in Michigan. The survey categorizes the activities into seven groups, including home-based work (HBWork), non-home-based work (NHBWork), home-based school (HBSchool), home-based shop (HBShop), home-based social (HBSocial), home-based other (HBOther), and non-home-based other (NHBOther). HBWork shows a trip directly from home to work or from work to home. NHBWork shows trips with one end at work while the other end is not home. HBSchool shows a trip from home to school or from school to home. HBShop shows a trip from home to shop or shop to home. HBSocial shows a trip from home to a recreational place or vice versa. HBOther shows a trip with one end at home while the other end is not in the previous groups. NHBWork shows a trip that has an end at work, but its other end is not home. NHBOther shows the trips that have no end at home or work. However, as mentioned before, in terms of EV applications, we need to distinguish between trips based on whether they originate from home/work or not (to consider higher availability of level 2 chargers at home/work). Thus, the defined seven activity types in the survey are categorized into four groups: HBWork, NHBWork, NHBOther, and the home-based non-work (HBNWork). Note that HBSchool, HBShop, HBSocial, and HBOther are combined in the latter group (HBNWork) since they all provide similar charging opportunities for users. The time-dependent probabilities for these four categories are then calculated by aggregating the survey results. These probabilities are then used to assign a trip purpose to each vehicle trajectory.

The other input to the simulation tool is the land use characteristics at the origin and destination of trips. The simulation tool focuses on three land use characteristics due to their impacts on charging behavior, namely residential (R), commercial (C), and other (O) and their area ratio (the ratio of the land use characteristic area over the total TAZ area) in zone k is denoted by $\mathcal{S}^1_k$, $\mathcal{S}^2_k$, and $\mathcal{S}^3_k$, respectively ($\mathcal{S}^1_k + \mathcal{S}^2_k + \mathcal{S}^3_k = 1$). Note that the last category, O, includes recreational, transport, and agricultural land uses. Thus, there are nine possible combinations of origin and destination zone types for each trip. The unadjusted static probability of origin (o)-destination (d) paired land use characteristics, ρ^{ij}_{od}, is defined as below:

$$\rho^{ij}_{od} = \mathcal{S}^i_o . \mathcal{S}^j_d \tag{1}$$

where i and j represents the land use characteristics. Assuming the purpose of each trip can be captured stochastically through its origin and destination land use, the nine possible combinations are crossed with the four sets of activities discussed earlier. Therefore, HBWork includes R—C and C—R, HBOther includes R—R, O—R, and R—O, NHBWork includes C—C, C—O, and O—C, and NHBOther includes O—O. Since the time-dependent distribution of each trip purpose (activity) is known, the origin-destination paired land use probabilities need to be adjusted according to their trip departure time intervals, using a temporal factor defined as follows:

$$\mathcal{T}^t_{od,m} = \frac{\mathcal{A}^t_m}{\sum_{ij} \chi^{ij}_m . \mathcal{S}^i_o . \mathcal{S}^j_d}. \tag{2}$$

where $\mathcal{T}^t_{od,m}$ is the temporal factor for activity m at time t for od and $\mathcal{A}^t_m$ is the time dependent share of activity. χ^{ij}_m is a binary parameter indicating if land use combination ij is a subset of m. The probability associated with each OD pair land use can be adjusted for each time interval by multiplying the defined temporal factor. The probability associated with each OD pair land use can be adjusted for each time interval by multiplying the defined temporal factor. Then, the origin-destination pair land use (thus associated trip purpose group) can be probabilistically assigned for each EV trajectory. To clarify this point, assume a hypothetical example as follows: Assume that HBWork share for a trip departure time interval is 0.55, shares of R and C land uses at the trip origin zone are 0.7 and 0.2, and shares of R and C land uses at the trip destination zone are 0.3 and 0.5. Then, the unadjusted probability associated with R—C and C—R would be $0.7 \times 0.5 = 0.35$, and $0.2 \times 0.3 = 0.06$, respectively. The temporal factor would be $(0.55/(0.35+0.06))$ and the adjusted probability for the trip to have R-C as the origin-destination paired land use would be $0.35 \times (0.55/(0.35 + 0.06))$.

Once the trip purpose, origin-destination paired land use characteristics, and residential type (if applicable) are assigned for each EV trajectory, using associated truncated random normal distributions, the initial and desired state of charge would be determined for the trajectory. The difference between the desired state of charge and the initial state of charge plus the charge spent en-route to reach the destination is the total charge required for each EV trajectory. If this value is positive, the EV would need to recharge along its path to the destination and its charging demand should be provided to the optimization model as an input; otherwise, the EV trajectory would not need recharging and would not be considered in the optimization model.

3.2. The mathematical optimization model

This section aims to present the developed modeling framework that minimizes the cost for providing the charging infrastructure, as well as the users' charging, queuing, and detour delays. The following notation is used in this study:

Sets	
$i \in I$	Set of zones
$\tau \in T$	Set of time intervals that vehicles get to charging stations
$\theta \in T$	Set of time intervals that vehicles leave charging stations

(*continued on next page*)

(*continued*)

$j \in J$	Set of electric vehicles that need recharging
Decision variables	
x_i	Binary decision variable for availability of a charging station at zone i which equals 1 if there is a charging station at zone i and zero otherwise
z_i	Integer decision variable for number of chargers to be provided at the charging station in zone$i$
State variables	
$Q_{ij}^{\tau\theta}$	Charging incidence matrix, which is one if EV j arrives to charging station in zone i at time interval τ and depart from it towards its destination at time interval θ
π_i^τ	Total charging and queuing delay experienced by EVs reaching to the charging station of zone i at time τ
TTd_j	Detour travel time required to reach the assigned charging station for EV j refueling
y_i^τ	Total number of EVs visiting the charging station at zone i at timeτ
v_i^τ	Total energy demand of EVs visiting charging station in zone i at timeτ
t_i^τ	Average remaining charging time for users at zone i at timeτ
μ_i^τ	Service rate of the charging station in zone i at time τ
λ_i^τ	Arrival rate to the charging station in zone i at timeτ
q_i^τ	Queuing time for the last vehicle joining the queue of the charging station in zone i at timeτ
χ_i^τ	Incidence matrix of observing queuing for the entire period of τ at the charging station of zone i. It is equal to one if there is a residual queue at the end of time interval τ, and zero otherwise.
δ_i^τ	Portion of time that queue length is greater than zero in charging station of zone i during time interval τ
$\overline{W}_i^\tau$	Average waiting time in charging station of zone i for EVs arriving at timeτ
R_{ij}	Refueling time for EV j recharging at the charging station of zone$i$
ρ_i^τ	Utilization rate of charging station zone i at timeτ
P_{i0}^τ	Probability of not having any vehicles using any chargers at charging station of zone i at timeτ
l_i^τ	Number of customers in the queue at charging station of zone i at timeτ
Parameters	
C_i^s	Cost of building and maintaining a charging station at zone i, converted to the depreciation cost per day (the assumed analysis period in the model formulation)
C_i^p	Cost of one charger installation and maintenance at zone i, converted to the depreciation cost per day
γ	Value of time
M	An arbitrary big number
E_{ij}^θ	Required energy for EV j to reach the charging station at zone i and depart from it toward its destination at time intervalθ
ζ_j	Desired state of charge for EV j at the destination
F	Maximum amount of charge that EVs can store
s_j	Initial state of charge for EVj
β	Battery performance
$d_{(a,b)}^c$	Distance between the centroid of zones a and b for vehicles departing at time c
s_{max}	State of charge that the charging speed drops beyond it
s_{min}	Minimum state of charge that drivers let their batteries drop to
$t_{(a,b)}^c$	Average travel time of vehicles departing zone a to destination zone b departing at time c
$t_j^{'}$	Departure time for EV j from its origin
t_j	Departure time interval for EV j from its origin
$O(j)$	Origin zone of EVj
$D(j)$	Destination zone of EVj
T_0	Duration of each time interval
α	Charging efficiency of batteries
P	Charging power
ε	An arbitrary small number

Three main assumptions are made to formulate the problem of interest in this study:

i. Users are assigned to paths and charging stations to minimize the total system cost.
ii. Detour of EVs for recharging does not affect network link travel times, i.e. EVs are not congestion makers, but congestion takers (Sheppard et al., 2017).
iii. Travel distances in urban networks are within the full range of EVs. Therefore, EVs that need recharging only recharge one time per route.
iv. The expected state of charging stations (average waiting times and charger occupancy rates) are known to the system.

In this study, we assume that the optimization models (especially the lower-level one) are implemented in different platforms (i.e., charging station apps), which not only provide routing guidance to users but also predict the queuing delay at each user's estimated future arrival time at various potential stations based on the availability of chargers and the best estimated demand. Such information can be updated dynamically, and then be disseminated to users to guide their route decisions.

The network considered in this study consists of a set of zones ($i \in I$). A set of time intervals ($\tau \in T$) at which EVs can arrive at charging stations. This discrete set allows the model to capture the visiting flow to stations over time. Another set of time intervals ($\theta \in T$) shows the time intervals at which vehicles depart the charging stations. This set enables the model to differentiate between the congestion levels in the arrival and departing time intervals. We assume T_0 is the duration of each time interval. Each electric vehicle

($j \in J$) has a trajectory that is known as a priori, with origin $O(j)$, destination $D(j)$, exact departure time $t_j^{'}$, departure time interval t_j, trip length $d^{t_j}_{(O(j),D(j))}$, travel time $t^{t_j}_{(O(j),D(j))}$, initial state of charge s_j, and desired state of charge at destination ζ_j. The solid line in Fig. 2 shows the shortest direct path from origin to destination.

If a lack of energy is an issue, the EV must recharge at one of the available charging station options ($I_n, n = 1 \cdots 4$). The EV will charge enough to reach its destination with its desired state of charge at destination (ζ_j). The energy required for EV j to reach to its destination, while visiting a charging station along its route and leaving it at time θ can be calculated as:

$$E^{\theta}_{ij} = \zeta_j F - s_j F + \frac{1}{\beta}[d^{t_j}_{(O(j),i)} + d^{\theta}_{(i,D(j))}], \quad \forall j \in J, i \in I \tag{3}$$

In the above formulation, F is the battery capacity, and β is the battery performance in$(\frac{mile}{kWh})$, which converts the energy to distance. Note that the inverse of this parameter $(\frac{1}{\beta})$, is the energy consumption rate per unit of distance $(\frac{kWh}{mile})$. While EVs' battery performances might differ based on the vehicle type and model, an average battery performance is considered for all EVs in the urban network. The required energy is calculated using the desired state of charge at destination, the initial state of charge and the distances from the origin zone to the charging zone, and from the charging zone to the destination zone. Having the charging demand, a micro-simulation-based model can be formulated as follows:

$$\min \sum_{i \in I}(C^s_i x_i + C^p_i z_i) + \gamma\left(\sum_{i \in I}\sum_{\tau \in T}\pi^{\tau}_i + \sum_{j \in J} TTd_j\right) \tag{4}$$

The objective function (4) consists of two main terms. The first term calculates the total infrastructure investment cost including the costs associated with the availability of charging stations, x_i, and the integer variable z_i that represents the number of chargers at each location i. The next term provides the monetary value of the total delay of all EV travelers that need recharging, including those related to the total queueing and charging delays, π^{τ}_i, at all charging stations for different arrival time intervals, as well as those related to the total detour time, TTd_j, experienced by EV users to access a charging station. These delays are multiplied by the value of time factor, γ, to calculate their monetary values. Please note that just an average value of time is considered for simplicity. This assumption can be easily updated and the research framework can be adjusted to capture the variations of value of time due to different classes of users, activities, and trip purposes. The objective function (4) is subject to constraints (5)–(18) and (21)–(27).

$$x_i \in \{0,1\}, \text{and} z_i \in \{0,1,2,\cdots\}, \quad \forall i \in I \tag{5}$$

$$z_i \le x_i M, \quad \forall i \in I \tag{6}$$

$$\sum_{\tau \in T}\sum_{\theta \in T} Q^{\tau\theta}_{ij} E^{\theta}_{ij} \le s_{max} F - s_j F + \frac{d^{t_j}_{(O(j),i)}}{\beta}, \quad \forall j \in J, i \in I \tag{7}$$

$$\sum_{i \in I}\sum_{\tau \in T}\sum_{\theta \in T} Q^{\tau\theta}_{ij} d^{t_j}_{(O(j),i)} \le \beta(s_j - s_{min})F, \quad \forall j \in J \tag{8}$$

$$\sum_{\tau \in T}\sum_{\theta \in T} Q^{\tau\theta}_{ij} \le x_i, \quad \forall i \in I, \forall j \in J \tag{9}$$

$$\sum_{\tau \in T}\sum_{\theta \in T}\sum_{i \in I} Q^{\tau\theta}_{ij} = 1, \quad \forall j \in J \tag{10}$$

$$TTd_j = \sum_{\tau \in T}\sum_{\theta \in T}\sum_{i \in I} Q^{\tau\theta}_{ij}(t^{t_j}_{(O(j),i)} + t^{\theta}_{(i,D(j))} - t^{t_j}_{(O(j),D(j))}), \quad \forall j \in J \tag{11}$$

$$t_j^{'} + t^{t_j}_{(O(j),i)} - T_0\tau \le \left(1 - Q^{\tau\theta}_{ij}\right)M, \quad \forall \tau \in T, \theta \in T, i \in I, j \in J \tag{12}$$

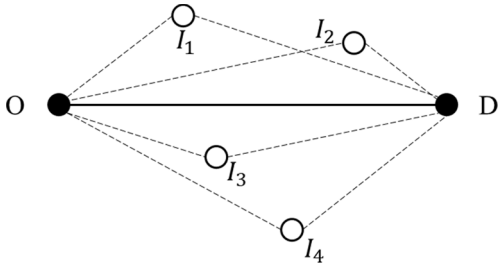

Fig. 2. An electric vehicle's route choices.

$$t_j^{'} + t_{(O(j),i)}^{tj} - T_0(\tau - 1) \geq \left(Q_{ij}^{\tau\theta} - 1\right)M, \quad \forall \tau \in T, \theta \in T, i \in I, j \in J \tag{13}$$

Constraint (5) states the binary decision variable to determine if a zone is equipped with a charging station ($x = 1$) or not ($x = 0$). Constraint (6) is a logical constraint ensuring that there is no charger in zone i if the zone does not have a charging station. Constraint (7) accounts for the maximum charge intake. It limits the charging incidence matrix by not letting the required charge exceed the available fast charging capacity in the battery at the time of arrival to the station. Constraint (8) ensures that each EV can only be charged in zones within its viable range. It should be noted that while the least energy level that EV users let their charge drop to is determined by s_{min}, the desired state of charge that they choose to have upon their arrival at a destination is determined by ζ_j. This value might be greater than s_{min} as a vehicle might need a higher state of charge for its subsequent trips. Constraint (9) ensures that charging can only happen when there is a charging station at zone i. Constraint (10) ensures that each EV charges exactly one time (note that the trajectories are filtered to the EVs requiring recharging). Constraint (11) calculates the detour travel time for each EV to get to the charging station. The detoured path travel time includes the average time-dependent travel time from the origin to the charging station and then to the destination. The original path travel time is the average travel time of vehicles with the origin of $O(j)$ and destination of $D(j)$. Constraints (12) and (13) are feasibility constraints that ensure vehicles can be allocated to a charging station upon arrival at the station.

$$y_i^{\tau} = \sum_{j \in J} \sum_{\theta \in T} Q_{ij}^{\tau\theta}, \quad \forall \tau \in T, i \in I \tag{14}$$

$$v_i^{\tau} = \sum_{j \in J} \sum_{\theta \in T} Q_{ij}^{\tau\theta} E_{ij}^{\theta}, \quad \forall \tau \in T, i \in I \tag{15}$$

Constraints (14) and (15) find the temporal charging demand for each station. Constraint (14) calculates the total number of EVs visiting the charging station of zone i at time τ, y_i^{τ}. Constraint (15) finds the required energy for all EVs visiting the charging station of zone i during time interval τ, v_i^{τ}. The arrival rate, λ_i^{τ}, which is the average number of EV users per charger visiting the station of zone i at time interval τ, is defined as:

$$\lambda_i^{\tau} = \frac{y_i^{\tau}}{T_0 z_i}, \quad \forall \tau \in T, i \in I \tag{16}$$

Similarly, the average charging time for a group of EVs visiting the charging station of zone i is denoted by t_i^{τ} and defined as:

$$t_i^{\tau} = \alpha \frac{v_i^{\tau}}{P y_i^{\tau}}, \quad \forall \tau \in T, i \in I \tag{17}$$

where P represents the charging power. The service rate, μ_i^{τ}, is defined as the number of EVs that can be charged in one hour and is calculated as follows:

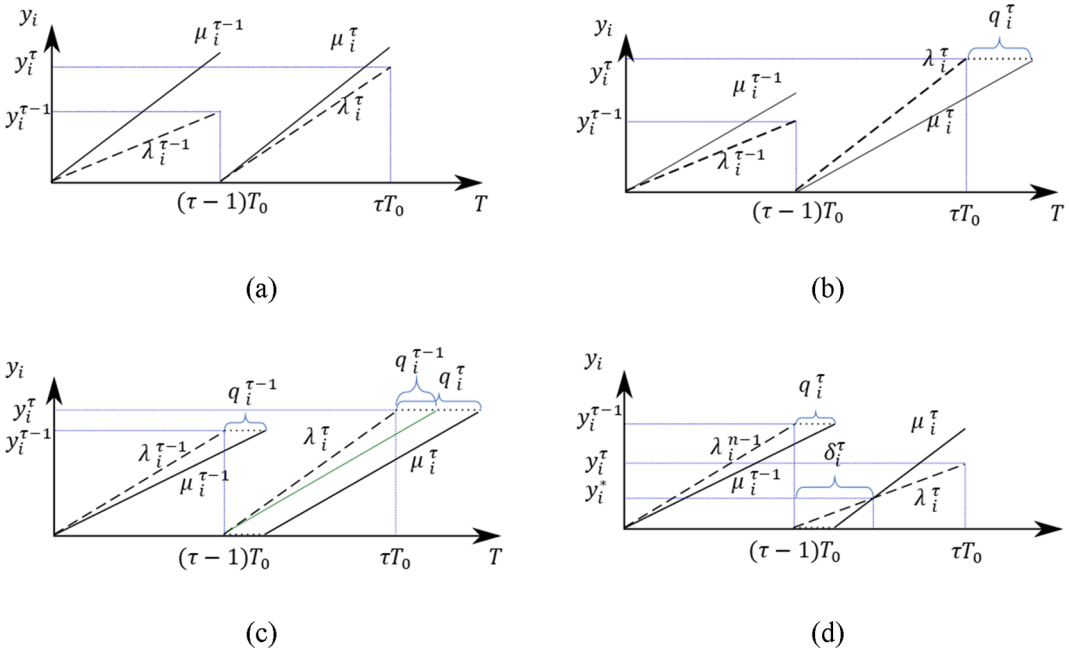

Fig. 3. Four queuing scenarios upon the arrival of EVs at charging stations.

$$\mu_i^\tau = \frac{1}{t_i^\tau}, \quad \forall \tau \in T, i \in I \tag{18}$$

The queueing delay at the end of time interval τ can be calculated as follows:

$$q_i^\tau = \frac{(\lambda_i^\tau - \mu_i^\tau)T_0}{\mu_i^\tau} + q_i^{\tau-1}, \quad \forall \tau \in T, i \in I. \tag{19}$$

Here, q_i^τ shows the longest waiting time experienced in station i at time interval τ. When EVs reach charging stations, four scenarios might occur depending on the remaining queue from the previous time interval, the arrival rate, and the service rate. These scenarios are illustrated in Fig. 3. If there is no remaining queue and the service rate is greater than the arrival rate, ($\mu_i^\tau > \lambda_i^\tau$), EVs experience no queue (Fig. 3a). If there is no remaining queue,($q_i^{\tau-1} = 0$), but the arrival rate is greater than the service rate, ($\mu_i^\tau < \lambda_i^\tau$), EVs experience queuing during the entire time interval (Fig. 3b). If there is a remaining queue form the previous time interval,($q_i^{\tau-1} > 0$), and the service rate cannot dissipate the queue by the end of the time interval, EVs experience queuing during the entire time interval (Fig. 3c). In this case, charging access cannot be provided to any incoming flow. Therefore, all vehicles will experience the queue and wait in line to get access to an available charger at a later time. In the last scenario (Fig. 3d), there is a remaining queue from the previous time interval but it dissipates before the end of the current time interval. Therefore, after a time, δ_i^τ, the incoming EVs can be charged upon their arrival. The value of δ_i^τ can be calculated as follows (see Appendix A for proof):

$$\delta_i^\tau = \frac{\mu_i^\tau q_i^{\tau-1}}{\mu_i^\tau - \lambda_i^\tau} \tag{20}$$

The above-mentioned deterministic queuing formulations can be summarized as follows:

$$q_i^\tau \geq \frac{(\lambda_i^\tau - \mu_i^\tau)T_0}{\mu_i^\tau} + q_i^{\tau-1} \tag{21}$$

$$q_i^\tau \geq 0, \quad \forall i \in I \tag{22}$$

$$q_i^0 = 0, \quad \forall i \in I \tag{23}$$

$$\frac{(\lambda_i^\tau - \mu_i^\tau)T_0}{\mu_i^\tau} + q_i^{\tau-1} \leq \chi_i^\tau M, \quad \forall \tau \in T, i \in I \tag{24}$$

$$\frac{(\lambda_i^\tau - \mu_i^\tau)T_0}{\mu_i^\tau} + q_i^{\tau-1} \geq (\chi_i^\tau - 1)M, \quad \forall \tau \in T, i \in I \tag{25}$$

$$\delta_i^\tau = T_0\chi_i^\tau + \frac{\mu_i^\tau q_i^{\tau-1}}{\mu_i^\tau - \lambda_i^\tau}(1 - \chi_i^\tau), \quad \forall \tau \in T, i \in I \tag{26}$$

$$\overline{W}_i^\tau = \frac{\delta_i^\tau}{T_0}\left(\frac{q_i^\tau + q_i^{\tau-1}}{2}\right), \quad \forall \tau \in T, i \in I. \tag{27}$$

Constraints (21)–(23) calculate the queuing delay at the end of each time interval. Constraint (21) sets a lower bound for the queuing delay by summing the queuing delay of the previous time interval and the additional queuing delay for the current interval. Constraint (22) ensures the estimated queue is always non-negative. Constraint (23) is a boundary condition assuming the system starts with no initial queue. Constraints (24) and (25) determine the type of queuing for time interval τ using the fully queued incidence matrix χ_i^τ. If the left-hand side of equation (24) is positive, resulting in a positive queue at the end of the time interval, the fully queued incidence matrix would be equal to one ($\chi_i^\tau = 1$). In this case, constraint (25) would not be binding. If the left-hand side of the constraint (25) becomes negative, the fully queued incidence matrix would be set to zero ($\chi_i^\tau = 0$). In this case, constraint (24) would not be binding. Constraint (26) calculates the portion of time interval with a queue. If the fully queued incidence matrix is equal to one, the second term of this constraint is zero and $\delta_i^\tau = T_0$. If the queue dissipates within the time interval, the first term will be zero and the second term calculates the δ_i^τ. Constraint (27) calculates the average queuing time for EVs visiting the charging station in zone i at time interval τ.

Finally, the following constraints provides the relationships among various time variables.

$$R_{ij}^\theta = \alpha\frac{E_{ij}^\theta}{P}, \quad \forall i \in I, j \in J \tag{28}$$

$$\pi_i^\tau = y_i^\tau \overline{W}_i^\tau + \sum_{\theta \in T}\sum_{j \in J} Q_{ij}^{\tau\theta} R_{ij}^\theta, \quad \forall \tau \in T, i \in I \tag{29}$$

$$t_j^{'} + t_{(o(j),i)}^{tj} + R_{ij}^\theta + \overline{W}_i^\tau - T_0\theta \leq \left(1 - Q_{ij}^{\tau\theta}\right)M, \quad \forall \tau \in T, \theta \in T, i \in I, j \in J \tag{30}$$

$$t_j^{'} + t_{(o(j),i)}^{t_j} + R_{ij}^{\theta} + \overline{W}_i^{\tau} - T_0(\theta - 1) \geq \left(Q_{ij}^{\tau\theta} - 1\right)M, \quad \forall \tau \in T, \theta \in T, i \in I, j \in J \tag{31}$$

Constraint (28) calculates the required time to recharge each EV at each charging station considering the loss of electricity factor and the charging power. Constraint (29) calculates the total delay in each charging station by summing up the total queuing delay for all EVs visiting the charging station at that time interval and the total refueling time of EVs for all departure time intervals from that station. Constraints (30) and (31) determine the departure time interval in which a vehicle would be able to leave the station. They ensure that the summation of the EV departure time, average travel time from origin to the charging station, the refueling time and waiting time in the queue matches the departure time interval from the station.

Note, in this mathematical modeling, only deterministic queuing is considered. In the next section the presented mathematical model is decomposed to two-subproblems. In the second subproblem the proposed solution approach accounts for both deterministic and stochastic queueing delays.

3.3. Solution methodology

The proposed Mixed-Integer Non-Linear Programming (MINLP) model in the previous section has multiple nonlinear constraints. The impact of queuing on the assignment of charging demands to charging stations, makes the problem highly nonlinear and challenging. In the literature, queuing time is usually considered only to determine the number of required chargers via a bi-level formulation or as a separate problem (Jung et al., 2014; Wang et al., 2019; Xie et al., 2018). Therefore, the proposed problem is decomposed into two subproblems assuming the queuing does not affect the assignment of charging demands to charging stations.

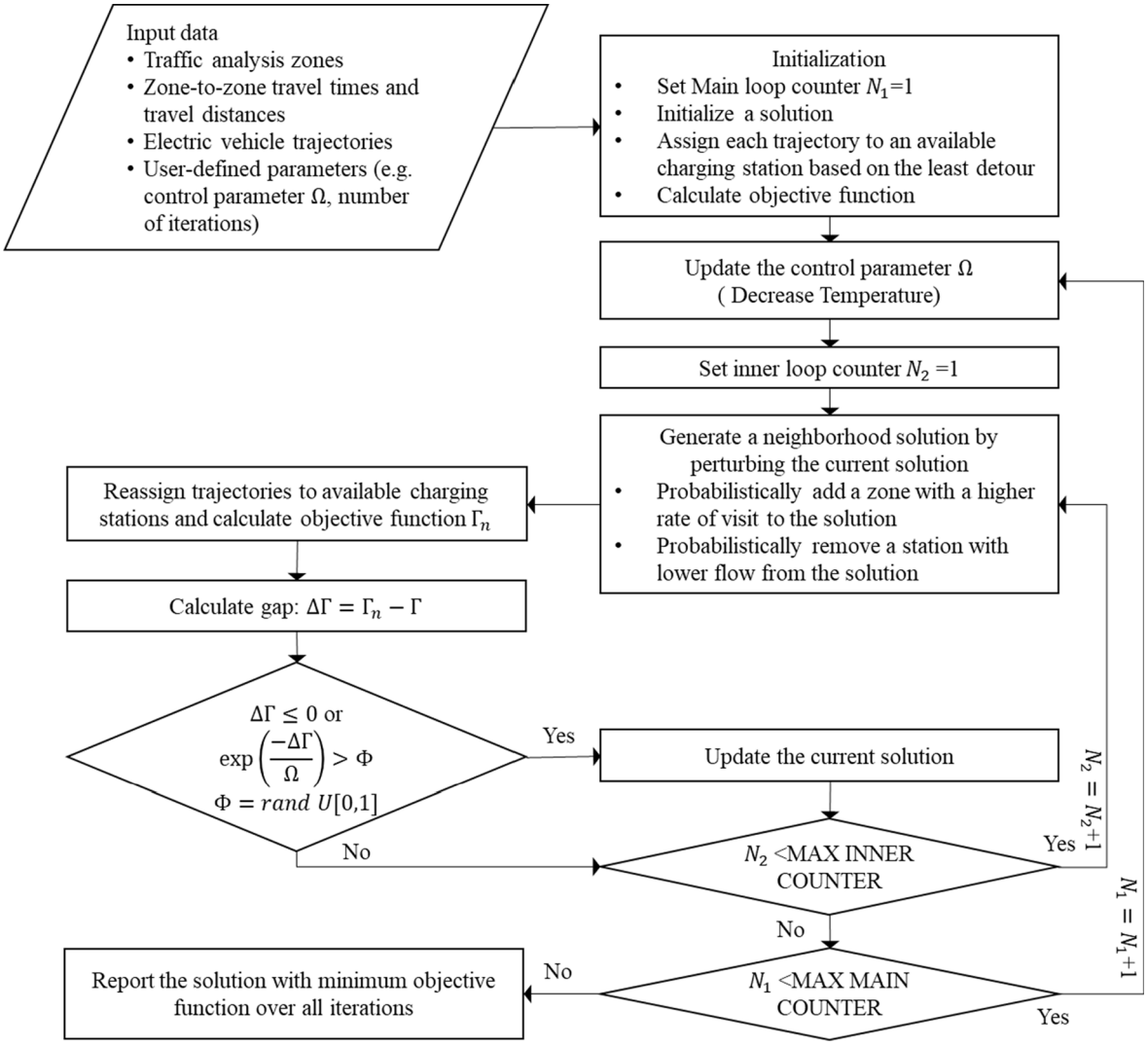

Fig. 4. The SA-based solution algorithm to find the optimal location of charging stations.

Since the decomposition approach is a heuristic approach, an implicit enumeration approach is compared with this approach for a small case study in the numerical experiments section to show its efficiency and accuracy. Note that the formulated problem is highly non-linear with mixed-integer variables. Thus, there is no exact solution methodology, and common commercial solvers cannot be implemented even for small case studies. Even in the decomposed approach, the first subproblem requires a heuristic approach for large scale applications.

3.3.1. Optimal locating of charging stations

In the first subproblem, a minimization problem is solved that considers the monetary value of detour and refueling times and the cost of charging stations, ignoring the charging queue. In this study, the number of chargers in each station is not limited, thus enough chargers would be provided at each station to provide a consistent level of service at each location, proportional to the charging demand. The mathematical model for the first subproblem, including the objective function and constraints, is as follows:

$$\min \sum_{i\in I}(C_i^s x_i) + \gamma\Big(\sum_{\tau\in T}\sum_{\theta\in T}\sum_{i\in I}\sum_{j\in J} Q_{ij}^{\tau\theta} R_{ij}^{\theta} + \sum_{j\in J} TTd_j\Big) \tag{32}$$

Subject to:
Constraints (5), (7)–(13), (28), and

$$t_j^{'} + t_{(O(j),i)}^{tj} + R_{ij}^{\theta} - T_0\theta \le \Big(1 - Q_{ij}^{\tau\theta}\Big)M, \quad \forall \tau \in T, \theta \in T, i \in I, j \in J \tag{33}$$

$$t_j^{'} + t_{(O(j),i)}^{tj} + R_{ij}^{\theta} - T_0(\theta+1) \ge \Big(Q_{ij}^{\tau\theta} - 1\Big)M, \quad \forall \tau \in T, \theta \in T, i \in I, j \in J \tag{34}$$

In this subproblem, the departure time confines the charging incidence matrix through constraints (33) and (34). In this model, the queuing delay in charging stations is ignored, unlike the primary optimization model. Therefore, per assumption, vehicles can be charged once they get to charging stations.

The objective function (32) along with its constraints form a mixed-integer linear model. Commercial solvers such as CPLEX and Gurobi, solve moderate sized instances effectively. However, as the size of the problem grows, the computational requirements increase exponentially. Therefore, a metaheuristic approach is also provided for large-scale case studies based on Simulated Annealing (SA) approach. For more details please refer to (Ghamami et al., 2020, 2016; Kavianipour et al., 2019; Zockaie et al., 2016) for similar applications of the SA algorithm.

To improve the efficiency of the algorithm, the following strategies are shown to be effective in generating neighboring solutions. More details of the algorithm can be found in Fig. 4.

1. To add a station randomly to a traffic analysis zone, each zone is weighted based on the number of crossing EV trajectories. Accordingly, the zones visited by a higher number of crossing trajectories, have a higher chance of being added to the current solution.
2. To remove a station randomly from traffic analysis zones equipped with one in the current solution, the zones are weighted based on the inverse of their number of incoming EV flows. Accordingly, stations with a lower incoming flow, have a higher chance to be removed from the current solution.

3.3.2. Optimal number of chargers at each charging station

To find the number of chargers in each charging station, the second subproblem is formulated as follows for each selected station in the first subproblem such as *i*:

$$\min C_i^p z_i + \gamma \sum_{\tau\in T} y_i^{\tau} \overline{W}_i^{\tau} \tag{35}$$

Subject to
(14)–(18) and (21)–(27)

The objective function (35) includes the total installation and maintenance costs of chargers, and the monetary value of total travelers' queuing delay at each station, which depends on the number of chargers allocated to the station. The objective function needs to be minimized for each charging station selected in the first subproblem, to find the optimum number of chargers, as the main decision variable. This problem is a MINLP.

In the first subproblem, EV trajectories requiring recharging are assigned to each charging station, forming a temporal arrival distribution for each charging station. Based on the availability of chargers at the station, they either charge upon their arrival or wait in the queue for an available charger. This subproblem makes a trade-off between providing more chargers or letting users wait in the queue for an available charger.

Assuming a uniform arrival and service rates for each time interval, the queuing behavior can be modeled based on a deterministic queue modeling approach (Zukerman, 2013), as presented in (21)–(27). The objective function (35) along with its constraints forms a mixed-integer problem with nonlinear constraints. Since the objective function is strictly convex (see Appendix B for the proof) and the constraints are convex, the proposed problem can be solved using numerical solution approaches such as the Golden-section search technique. This technique is designed to find the extreme value of a function in a pre-defined interval as its domain (Kiefer, 1953). The deterministic queuing assumption provides the minimum number of chargers required to support the charging demand.

The deterministic queueing model, which assumes uniform arrival and service rates, results in zero queueing delay when the service rate is greater than the arrival rate. Thus, if enough chargers are provided to avoid the deterministic queue, the service rate would be greater than the arrival rate. However, if the arrival of vehicles to the charging station is assumed to follow a Poisson distribution and service rates distributions are assumed to be exponential, then there is a chance for queuing even when the service rate is greater than the arrival rate (Zukerman, 2013). It should be noted if the arrival rate is greater than the service rate, only the deterministic approach is applicable. If a steady-state condition is assumed in each time interval, the M/M/k (M stands for Markovian, which is a Poisson distribution for arrival rates and an exponential distribution for service time distribution and k represents multiple number of chargers) queuing model can be used to model the stochastic queuing delay. The formulation is as follows:

$$\rho_i^\tau = \frac{\lambda_i^\tau}{z_i \mu_i^\tau}, \quad \forall \tau \in T, i \in I \tag{36}$$

$$P_{i0}^\tau = \left(\sum_{m=0}^{z_i-1} \frac{(z_i\rho_i^\tau)^m}{m!} + \frac{(z_i\rho_i^\tau)^{z_i}}{z_i!(1-\rho_i^\tau)}\right)^{-1}, \quad \forall \tau \in T, i \in I \tag{37}$$

$$I_i^\tau = \frac{P_{i0}^\tau \left(\frac{\lambda_i^\tau}{\mu_i^\tau}\right)^{z_i} \rho_i^\tau}{z_i!(1-\rho_i^\tau)^2}, \quad \forall \tau \in T, i \in I \tag{38}$$

$$\overline{W}_i^\tau = \frac{I_i^\tau}{\lambda_i^\tau}, \quad \forall \tau \in T, i \in I \tag{39}$$

In these formulations, Eq. (36) finds the utilization, ρ_i^τ, at each charging station in each time interval. Eq. (37) finds the probability that there is no queue in the system. Eq. (38) finds the number of customers in the queue. Finally, equation (39) calculates the average waiting time in the queue. These equations are based on queuing theory for M/M/k queues. For more information on queuing theory, please refer to Zukerman (2013). The average queue size of the M/M/k system is convex with respect to the traffic flow (Grassmann, 1983). Therefore, the optimum value of the objective function can be calculated using the Golden-section search technique similar to the deterministic approach. The two-stage framework for finding the optimal number of chargers considering both deterministic and stochastic approaches is presented in Fig. 5. Note that the deterministic model provides a lower bound for the stochastic model, without which the Golden-section method cannot be applied to the stochastic model. Furthermore, in case of a non-zero deterministic queue in the first stage, the stochastic queueing model would be irrelevant.

4. Numerical experiments

This section first introduces the case studies and their network specifications. Then, it provides the input data used in the charging behavior simulator. Next, it briefly discusses the considered parameter values in the optimization model. It is worth noting these values

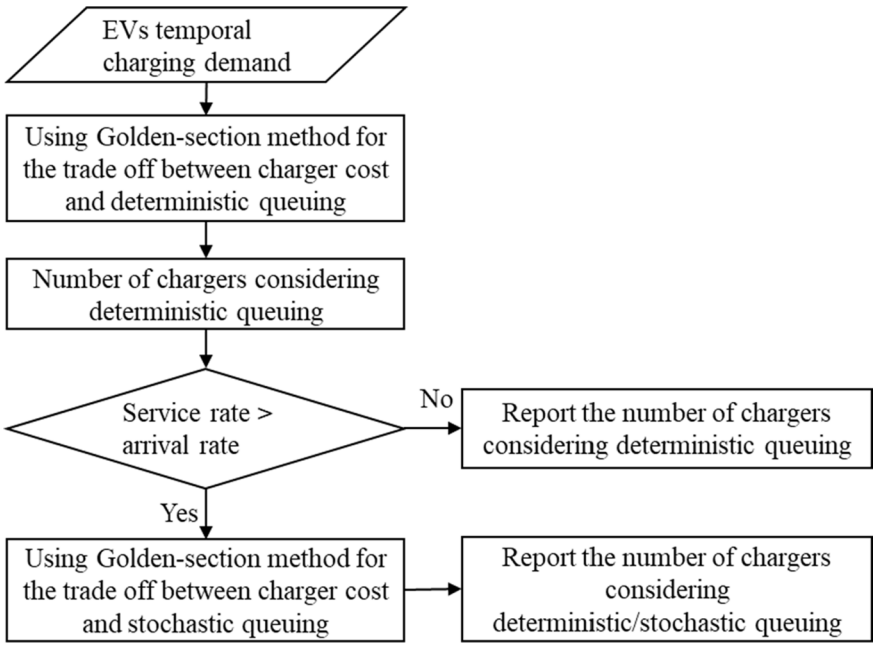

Fig. 5. Two-stage framework for finding the optimal number of chargers considering deterministic and stochastic queuing delays.

are derived based on the provided feedback in stakeholder meetings in Michigan and can be calibrated for each region based on the input from various stakeholders' meetings as part of the EV charger placement project in Michigan. Finally, some scenarios are introduced to be accompanied by sensitivity analyses to provide applied insights for the EV fast-charging infrastructure deployment in urban areas.

4.1. Case studies

The road network and OD travel demand information in the State of Michigan are provided by MDOT. The regional road networks for the cities of Marquette, Lansing and Detroit are extracted, as shown in Fig. 6, beyond the actual city borders. The city of Marquette is considered as a small-sized network which has 62 nodes, 21 zones, and 336 lane-miles in length. The city of Lansing is considered as a medium-sized network with 896 nodes, 91 zones, and 2,030 lane-miles in length. The city of Detroit is the large-scale network used in this study, which has 5,461 nodes, 301 zones, and 8,776 lane-miles in length.

The land use information is provided by MDOT for each traffic analysis zone in the state-wide network. The land acquisition costs are provided for each traffic analysis zone by city municipalities. Utility provision costs are provided through utility companies serving these three cities (DTE Energy and Consumers Energy). Two levels of powers are considered for charging stations: 1) 50 kW with a

Fig. 6. (a) Michigan state-wide network. (b) City of Marquette case study network. (c) City of Lansing case study network. (d) City of Detroit case study network.

station cost of $48,437 and a charger cost of $33,750, 2) 150 kW with a station cost of $80,125 and a charger cost of $76,250. Two battery sizes of 70 kWh and 100 kWh are considered for EVs. The battery performance is assumed to be 3.5 mi/kWh (with an energy consumption rate of 0.3 kWh per mile) during the summer, with a 30% reduction for winter weather conditions (the latter is considered as the critical case for Michigan). The data were obtained through various stakeholder meetings from car companies (i.e., Ford, GM, etc.) An EV adoption rate of 6% is considered, which means that 6% of total trajectories are by EVs, based on the projected 2030 EV market share in Michigan by MISO Energy (MISO Energy, 2018). A value of time of $18/h is used to monetize traveler delay. The combination of the two battery capacities and charger powers leads to four scenarios, which are investigated for each city in the next section.

In this study, the initial state of charge (as a fraction of the EV battery capacity) before noon is assumed to follow a normal distribution with the average and standard deviation values presented in Table 1. It is worth noting that these values are based on the current circumstances in Michigan. For the trips departing between noon and 5:00 PM, the mean values are assumed to be reduced by 0.1. For trajectories departing after 5:00 PM, another 0.1 reduction is implemented. Moreover, a normal distribution with a mean of 0.15 and a standard deviation of 0.1 is considered for the desired state of charge for EVs at their destination.

4.2. Results

In this section, we first explore various aspects of the solution methodology to demonstrate the performance of the proposed approach (i.e. validation of the decomposition approach for the main problem, comparison of the metaheuristic approach with the commercial solver for the first subproblem, and comparison of the deterministic and stochastic queuing models in the second subproblem). Then, the results are provided for the four defined scenarios in two large case studies.

4.2.1. Enumeration versus decomposition

To test the performance of the decomposition approach, i.e., its solution quality and convergence speed, we compare it with a simple enumeration approach which exhausts all facility combinations. Since such a simple approach cannot be applied even to small-sized networks, a subset of zones is selected as candidate locations for the charging stations in the smallest case study, Marquette network. We test an application with five randomly selected zones (out of 21 zones) to be candidates for charging stations.

First, the dynamic traffic assignment tool, DYNASMART-P, uses the dynamic OD demand table to simulate traffic and generate vehicle trajectories. Then, the charging behavior simulation takes the trajectories from the dynamic traffic assignment tool and assigns initial/desired SOC for each trajectory considering its departure time, land use characteristics at origin/destination, and residential type (if applicable). Note that in addition to the dynamic traffic demand, different time-dependent distributions are considered for the initial/desired SOC based on the trip departure time. Considering 70 kWh batteries, 197 EV trajectories need to recharge to fulfill their trips in city of Marquette. This charging demand is the input to both decomposition and explicit enumeration approaches. To make the enumeration approach traceable, first the decomposition problem is solved, then the enumeration set is defined accordingly using the decomposition solution to generate an upper bound solution. To solve the problem using the decomposition approach, this demand is provided to its first subproblem which finds the location of charging stations. The first subproblem is solved using a commercial solver, CPLEX, and suggests four charging stations, i.e., $x = [1,0,1,1,1]$. The second subproblem needs to be solved for each selected charging station to determine the number of chargers within them. As the first subproblem suggests four charging stations, the second subproblem is solved four times, once for each selected candidate location in the first sub-problem. The location of charging stations and the number of chargers within each charging station is the output of the decomposition approach. The decomposition approach solution includes a maximum of three chargers among the selected candidate locations, i.e., $z = [3, 0, 2, 2, 2]$. The result of the decomposition approach needs to be verified, which is accomplished by comparing it against the explicit enumeration. In this approach, the objective function value of the main problem is calculated for all possible combinations of charging stations and chargers. The maximum number of required chargers at each station should not be bounded in theory, but failure to set a cap on the maximum number of chargers prevents exhausting all combinations. Therefore, a subset of scenarios needs to be considered. Since the solution from the decomposition approach uses a maximum of three chargers over the different locations, we set the maximum number of chargers per station to four in our enumerations (assuming building four chargers at each candidate location as an upper bound solution). In this case, each candidate location can have zero, one, two, three, or four chargers, yielding five different settings for each candidate charging station. If a location is associated with at least one charger, a station must also be available there. On the other hand, zero charger at a candidate location will mandate that no charging station is built there, and no traveler will be assigned by the commercial solver to that candidate location. The total number of combinations can be calculated as below.

Table 1
Parameters of normal distributions for the initial state of charge.

Battery (kWh)	Initial state of charge (% battery)			
	70		100	
	Mean	SD	Mean	SD
Home- single family	0.75	0.05	0.7	0.05
Home- multi family	0.5	0.2	0.6	0.2
Work	0.6	0.2	0.65	0.3
Other	0.55	0.3	0.6	0.3

$$N_c = (N_s)^{N_l} \tag{40}$$

where N_c is the total number of combinations, N_l is the number of candidate locations, and N_s is the number of settings that chargers can have in each candidate charging station. Therefore, the total number of possible charger installation combinations is equal to 5^5. For each of these combinations, the assignment of charging demand to available charging stations is solved using Knitro, and the objective function is evaluated. The combination with the minimum objective function value suggests a maximum of three chargers, i.e., $z = [3, 0, 2, 1, 2]$, and does not reach the cap of four chargers. This solution is compared with the solution of the decomposition approach in Table 2, which also provides results for an application with seven randomly selected zones as an alternative application to quantify the impacts of the problem size on the solution time for the enumeration approach. Fig. 7 shows the number of combinations, 5^7, which should be tested for this application. In this figure, each box represents a candidate location, and each value represents the number of settings that each candidate location may take for number of chargers. Note that the optimization problem finds the number of chargers for each candidate location. However, in Table 2 only the total number of chargers over different locations is reported to be consistent with the larger case studies, where the location-specific number of chargers cannot be provided in tables.

For the application with seven candidate locations, both approaches suggest a similar solution, i.e., $z = [4, 0, 0, 2, 1, 0, 2]$, and provides the same objective function. The results show the decomposition technique provides a solution that is very close to, or identical to, the optimal solution (within zero or one percent difference). However, the solution time is much faster. Since the number of facility combinations grows exponentially with the network size (e.g., number of candidate zones), it is impossible to solve the full-scale problem even for small case studies via the enumeration approach. In contrast, the decomposition approach can provide a near-optimum solution instantaneously for this small case study.

4.2.2. Robustness

This section studies the impact of seed numbers on the optimum solution. Seed numbers determine the random number generation, affecting the simulated users' charging behavior since the initial and desired SOC are determined based on random numbers. Thus, the impact of ten different seed numbers, i.e., scenarios, are studied in the medium-sized network (city of Lansing). The objective function, number of stations, and number of chargers are compared in these scenarios. Fig. 8a shows the objective function values vary by almost 3 percent in these scenarios, which shows the availability of almost identical solutions with different representations. Fig. 8b shows most of the scenarios have 16 charging stations, while the highest number of charging stations is 18, which indicates the number of stations is quite stable over different scenarios. Our solution shows only about 16–18 built charging stations in about 94 TAZs (as a result of cost-benefit trade-offs). Note that TAZs are defined as candidate locations to be equipped with charging stations. Thus, there will be, at most, one charging station at each TAZ. This is a justified assumption considering the role of TAZs in defining network travel demand.

Lastly, Fig. 8c shows the number of chargers at each TAZ across all scenarios, where each (non-zero) spike indicates the installation of a charging station at that location. Since the jumps are typically occurring at the same locations, it shows that location of charging stations is almost the same for all scenarios. Thus, it can be concluded that in addition to the number of charging stations, the spatial distribution of the stations is also fairly stable across the random scenarios. Furthermore, according to Fig. 8c, the number of chargers and their spatial distribution change only slightly (which is expected because of the charging demand variations across random realizations). The charging demand in different charging stations varies from one scenario to another, due to changes of spatial distribution of EV trajectories that require charging in various scenarios with different seed numbers. While the differences in scenarios are small, the solution robustness can be improved by considering multiple random seeds for random number generation and applying the proposed framework for each scenario. Since the focus of the study is to develop the framework, the numerical experiments are performed for one seed number.

4.2.3. CPLEX versus simulated Annealing

We further test the SA approach for the first subproblem (i.e., locating charging stations). Fig. 9 shows the convergence of the metaheuristic approach for the city of Lansing toward the optimal value provided by CPLEX. It shows that the objective function of the metaheuristic approach can get very close to the optimal solution. The solution quality of the metaheuristic approach is evaluated for

Table 2
Comparing the enumeration and decomposition technique for a small network.

Scenario	5 Candidate Stations			7 Candidate Stations		
Technique	Enumeration	Decomposition	Percent Difference	Enumeration	Decomposition	Percent Difference
Number of Stations	4	4	0.0%	4	4	0.0%
Number of Chargers	8	9	12.5%	9	9	0.0%
Average Charging delay (min)	15.73	15.82	0.6%	15.31	15.31	0.0%
Average detour delay (min)	5.84	5.75	−1.5%	4.51	4.51	0.0%
Station Cost (m$)	0.56	0.56	0.0%	0.56	0.56	0.0%
Chargers Cost (m$)	0.29	0.32	12.5%	0.32	0.32	0.0%
Infrastructure Cost (m$)	0.84	0.88	4.2%	0.88	0.88	0.0%
Total objective function value ($/day)	1511	1520	0.6%	1417	1417	0.0%
Solution time (s)	12,600	4	−100.0%	241,200	4	−100.0%

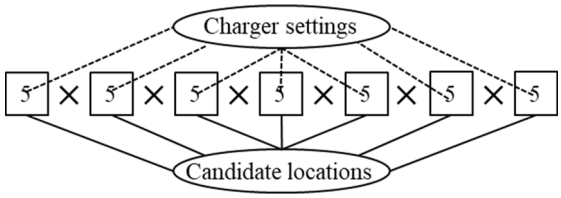

Fig. 7. Permutation of available combinations for enumeration approach.

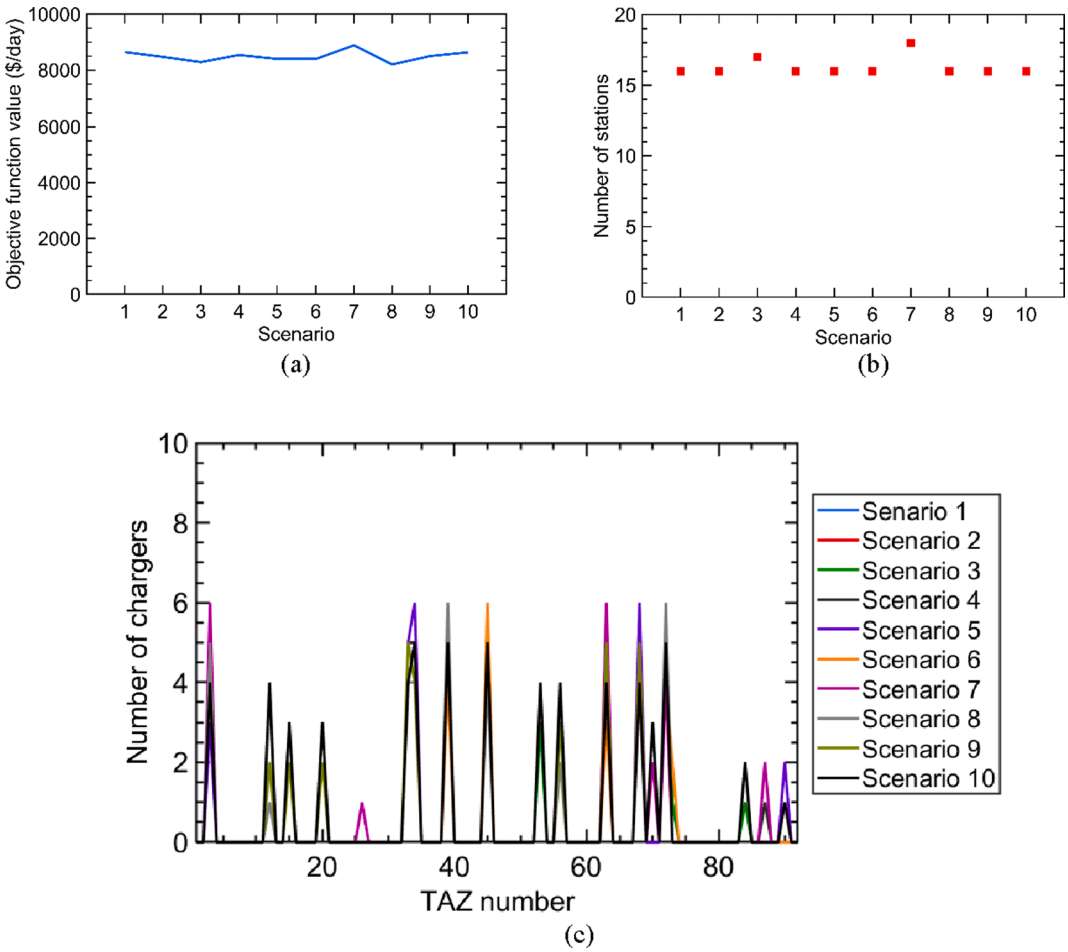

Fig. 8. The impact of seed number on the (a) optimum objective function value (b) number of stations (c) Number of chargers at each TAZ for city of Lansing.

the city of Lansing and Detroit in Table 3. Although the optimum objective function value for the first subproblem increases by 1.5% and 2.4% for the two cities, the computational efficiency in terms of the required memory is decreased significantly by 84% and 96%, respectively. Furthermore, the solution time of the metaheuristic approach is reduced by a 30% margin for the medium-size case study, and over 50% for the large-scale case study. One should note the problem size is almost tripled in terms of the number of zones from Lansing case study to Detroit case study. However, the memory requirement is increased by a factor of 20. This shows the importance of the metaheuristic approach for even larger case studies.

Furthermore, the charging station configurations at the network level are provided in Fig. 10. The red dots represent installed charging stations, while the blue dots show candidate locations that have not been selected. The size of each red dot represents the recommended number of chargers. The size of the traffic analysis zones increases as the population density decreases. Fig. 10 shows that the locations of charging stations are almost the same in both approaches.

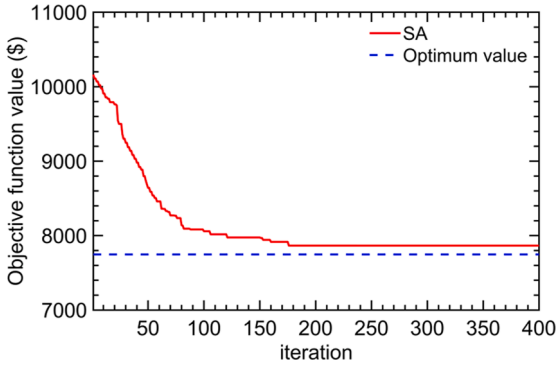

Fig. 9. The convergence of the metaheuristic method toward the optimal objective function provided by CPLEX for the city of Lansing.

Table 3
Comparing CPLEX and SA performance in solving station location subproblem.

City	Lansing			Detroit		
Technique	CPLEX	SA	Percent difference	CPLEX	SA	Percent difference
Battery size (kWh)	70	70	–	70	70	–
Charging station (kW)	50	50	–	50	50	–
Number of zones	92	92	–	301	301	–
EV Trajectories	28,574	28,574	–	212,299	212,299	–
Number of Stations	16	16	0.0%	62	62	0.0%
Number of Chargers	87	92	5.7%	641	639	−0.3%
Average delay (min)	10.75	10.93	1.7%	11.19	11.37	1.6%
Station Cost (m$)	2.52	2.66	5.3%	15.37	15.37	0.0%
Chargers Cost (m$)	3.48	3.30	−5.2%	23.22	23.15	−0.3%
Infrastructure Cost (m$)	6.00	5.95	−0.8%	38.59	38.52	−0.2%
Charging station location subproblem objective function value ($/day)	7,747	7,860	1.5%	67,543	69,193	2.4%
Total objective function value ($/day)	8,803	8,858	0.6%	74,507	76,118	2.2%
Required memory (GB)	5.20	0.82	−84.2%	107	4.2	−96.1%
Solution time (s)	323	238	−26.3%	16,717	8311	−50.3%

4.2.4. Deterministic versus stochastic queueing models

Deterministic queuing provides a zero queuing time when the service rate exceeds the arrival rate. In this case, a steady state stochastic queuing, which does not exist when the service rate is smaller than arrival rate, can be applied. Fig. 11 compares the deterministic queueing model with an M/M/k model for a sample charging station, and provides the values of the two-stage model. Note that the deterministic model provides a left bound (minimum number of chargers that certify higher service rate relative to the arrival rate) for the stochastic model, without which the Golden-section method cannot be applied to the stochastic model. The figure plots the objective function value relative to the number of chargers for each stage. The objective function of the stochastic queuing can be determined when the service rate is higher than the arrival rate, as reflected in Fig. 11. As it is shown, a greater number of chargers is required to count for the stochastic queueing delay, in addition to the deterministic queueing delay.

For Lansing and Detroit, four scenarios are investigated based on battery capacity and charging power. Table 4 summarizes the model output. Consideration of 150 kW chargers provides a lower total investment cost despite a higher unit cost for these chargers (Kavianipour et al., 2021). Furthermore, they provide lower charging and queuing times for travelers. Meanwhile, the 70 kWh vs. 100 kWh battery scenarios demonstrate a slight reduction in the number of charging stations under the larger battery size, as expected. However, the total number of chargers remains almost the same. The main reason for this observation may be caused by the fact that the charging behavior simulation tool uses various distributions for the initial and desired states of charge as a fraction of the battery size. This is a different pattern relative to a recent study (Ghamami et al., 2020) for intercity networks (which is different in nature to urban areas).

5. Conclusion

This study develops a methodological framework to find the optimum investment plan for building a network of charging stations for urban areas considering queueing delays and feasibility of EV trips. This study finds the locations for charging stations and the number of chargers at each location, with an approximate cost of building such networks. A charging behavior simulator tool is developed and used along with a traffic simulation tool to provide simulated user charging demand as the main input. No study in the literature captures all of these features for urban areas. The optimization model is decomposed into two subproblems. The first subproblem finds the location of the charging stations, and the second subproblem finds the required number of chargers at those

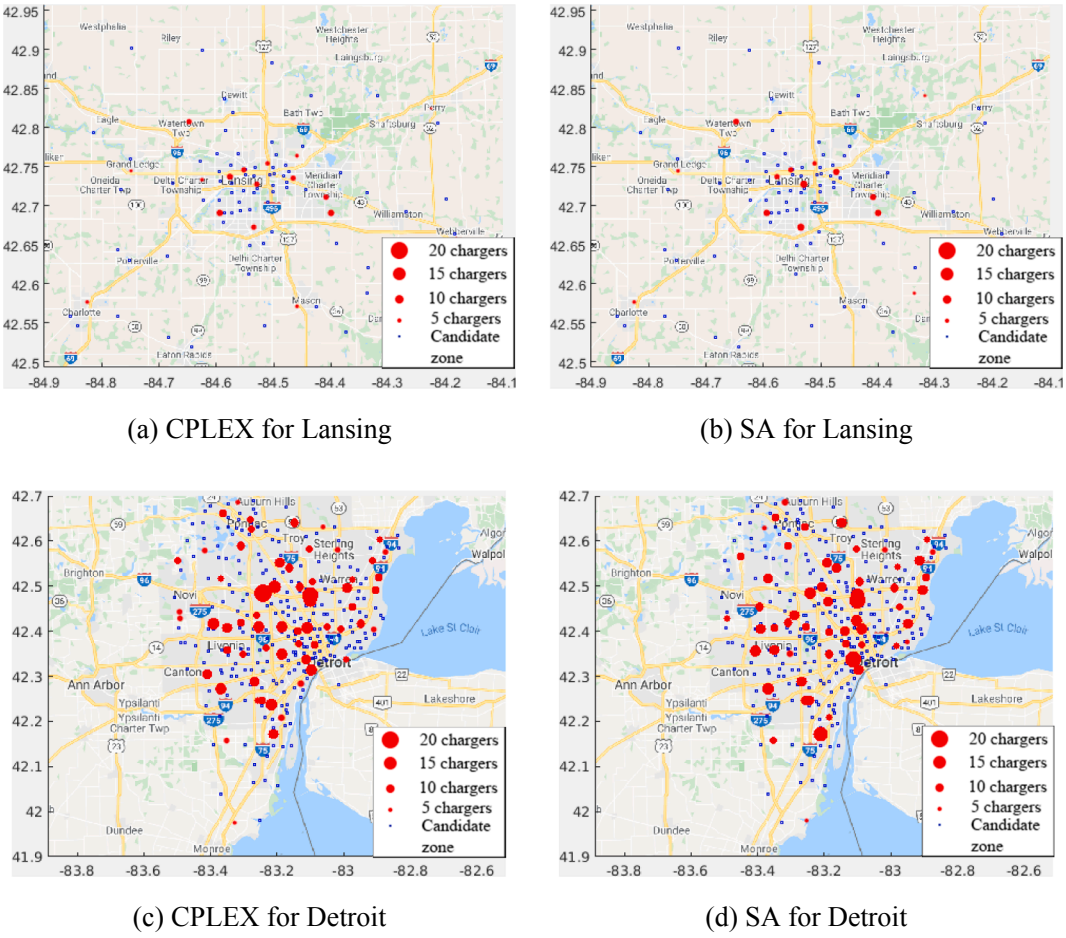

Fig. 10. Charging station configurations for the cities of Lansing and Detroit with CPLEX and SA algorithm.

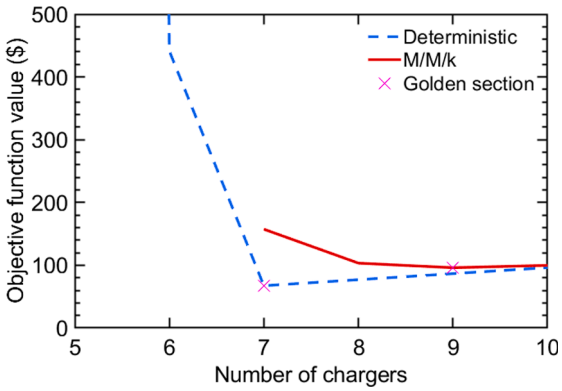

Fig. 11. The optimum number of chargers for a sample charging station considering deterministic and stochastic queuing models.

stations. The former is solved using two approaches, a metaheuristic algorithm and using commercial solvers. The latter is solved using the Golden-section method via a two-stage algorithm that captures both deterministic and stochastic queueing delays. The methodology is first validated for a small case study in the city of Marquette. Then, the research approach and results are presented for two urban areas in Michigan, namely the cities of Lansing and Detroit, to ensure the feasibility of the urban trips of EV users in those regions by 2030 under a predicted market share. The winter scenario with 70 percent battery performance is tested under battery energy levels of 70 kWh and 100 kWh, and charger power levels of 50 kW and 150 kW.

The results of the tested scenarios provide the key findings as follows:

Table 4
Comparing the optimum solutions under various battery capacity and charger power for the cities of Lansing and Detroit.

City	Lansing				Detroit			
Battery size (kWh)	70	100	70	100	70	100	70	100
Charging power (kW)	50	50	150	150	50	50	150	150
Number of zones	92	92	92	92	301	301	301	301
# EV trajectories	28,574	28,574	28,574	28,574	212,299	212,299	212,299	212,299
# of stations	16	14	13	10	62	51	52	40
# of chargers	85	89	36	33	639	618	239	228
Station cost (Million dollar)	2.52	2.21	2.47	1.88	15.37	12.64	14.54	11.18
Charger cost (Million dollar)	3.39	3.56	2.96	2.73	23.15	22.39	18.82	17.95
Total infrastructure cost (Million dollar)	5.91	5.78	5.43	4.62	38.52	35.03	33.35	29.13
Average charging and queuing delay (min)	10.8	14.74	3.83	5.26	11.37	15.29	3.98	5.30

- The decomposition approach provides near-optimum solution to the main problem (within one percent of the optimal solution provided by the enumeration approach) in the small case study.
- 150 kW chargers reduce the charging and waiting time for travelers, as compared to that of 50 kW chargers.
- Due to the higher throughput of 150 kW chargers, the number of 150 kW chargers needed to support the EV trips in urban areas is much smaller than that of 50 kW chargers. Therefore, implementing a network of 150 kW chargers is less costly despite the higher per unit cost of these chargers.
- The battery size does not affect the number of chargers in urban areas, unlike the intercity network, as the length of the urban trips is significantly lower than the range of EVs.

The presented numerical results are provided based on the estimated input parameters via several meetings with various stakeholders. This provides applied insights for planning agencies on appropriate estimates for the required infrastructure investment to support EV trips in urban areas. However, this study incorporates the market share as a given input. It is expected that the market acceptance of EVs be affected by the available charging infrastructure. Thus, capturing the endogeneity of the market share and the charging infrastructure at the network level is one of the main future research directions. Further, incorporating trip chain data and adjusting the model accordingly is an important future research direction. Another future path to consider is the impact of vehicle type and model on the battery performance and capacity.

Acknowledgments

This material is based upon work supported by the Department of Energy and Energy Services under Award Number EE008653. The authors also appreciate the assistance of the Bureau of Transportation Planning staff at the Michigan Department of Transportation (MDOT) in making data available to the study, especially Bradley Sharlow and Jesse Frankovich. The authors naturally remain solely responsible for all contents of the paper.

Appendix A

Based on Fig. 3d, y_i^* can be derived as follows:

$$y_i^* = \delta_i^\tau \lambda_i^\tau \tag{41}$$

$$y_i^* = \left(\delta_i^\tau - q_i^{\tau-1}\right)\mu_i^\tau \tag{42}$$

$$\delta_i^\tau \lambda_i^\tau = \left(\delta_i^\tau - q_i^{\tau-1}\right)\mu_i^\tau \rightarrow \delta_i^\tau \lambda_i^\tau - \delta_i^\tau \mu_i^\tau = -q_i^{\tau-1}\mu_i^\tau \tag{43}$$

$$\rightarrow \delta_i^\tau\left(\mu_i^\tau - \lambda_i^\tau\right) = \mu_i^\tau q_i^{\tau-1} \rightarrow \delta_i^\tau = \frac{\mu_i^\tau q_i^{\tau-1}}{\mu_i^\tau - \lambda_i^\tau} \tag{44}$$

Appendix B

If the objective function and feasible set is convex, then the problem has a unique solution and the Golden-section method can be applied to solve the problem.

First, we examine the objective function:

$$\Gamma = C_i^p z_i + \gamma \sum_{\tau \in T} y_i^\tau \overline{W}_i^\tau = C_i^p z_i + \sum_{\tau \in T} y_i^\tau \frac{\delta_i^\tau}{T_0}\left(\frac{q_i^\tau + q_i^{\tau-1}}{2}\right) \tag{45}$$

In the above formulation, $C^p$and γ are parameters and y_i^τ is known as it is the output of the location subproblem. Based on the constraint (26), δ_i^τ is a function of $\chi_i^\tau$and z_i. q_i^τ is also a function of χ_i^τ, z_i, and $q_i^{\tau-1}$.

Inductive reasoning can be used to show the convexity of q_i^τ as follows:

Step 1: The convexity of q_i^τ should be checked for $\tau = 1$.

$$q_i^\tau = \frac{(\lambda_i^\tau - \mu_i^\tau)T_0}{\mu_i^\tau}\chi_i^\tau \tag{46}$$

$$\text{If } \chi_i^1 = 0 \rightarrow q_i^1 = 0 \rightarrow Convex \tag{47}$$

$$\text{If } \chi_i^1 = 1 \rightarrow q_i^\tau = \frac{\left(\frac{y_i^\tau}{T_0 z_i} - \mu_i^\tau\right)T_0}{\mu_i^\tau} \rightarrow \frac{d(q_i^\tau)}{dz} = -\frac{y_i^\tau}{\mu_i^\tau z_i^2} \rightarrow \frac{d^2(q_i^\tau)}{dz^2} = 2\frac{y_i^\tau}{\mu_i^\tau z_i^3} = 2\frac{y_i^1}{\mu_i^1 z_i^3} \tag{48}$$

(47) and (48) are both convex, which shows the convexity of the q_i^τ for $\tau = 1$.

Step 2: It is assumed that q_i^τ is convex for $\tau = n-1 \rightarrow q_i^{n-1}$ is convex.

Step 3: The convexity of q_i^τ should be checked for $\tau = n$

$$q_i^n = \chi_i^n\left(\frac{T_0}{\mu_i^n}\left(\frac{y_i^n}{T_0 z_i} - \mu_i^n\right) + q_i^{n-1}\right) \tag{49}$$

$$\text{If } = 0 \rightarrow q_i^n = 0 \tag{50}$$

$$\text{If}\chi_i^n = 1 q_i^n = \frac{T_0}{\mu_i^n}\left(\frac{y_i^n}{T_0 z_i} - \mu_i^n\right) + q_i^{n-1} \tag{51}$$

(50) is convex. (51) consists two terms: the first is convex similar to (48) and the second term is convex per assumption in step 2. Therefore, the convexity of q_i^τ can be concluded based on inductive reasoning.

The next step is to prove the convexity of the objective function. The objective function is a function of z_i and $\chi_i^n, n = 1, \cdots \tau$. The first part of the objective function is convex. Therefore, the second part is evaluated for convexity as follows:

$$\Gamma^{'} = \gamma\sum_{\tau\in T} y_i^\tau \overline{W}_i^\tau \tag{52}$$

The convexity of $y_i^\tau \overline{W}_i^\tau$ is similar to the convexity of $\Gamma^{'}$(Boyd and Vandenberghe, 2009).

$$\Gamma'' = y_i^\tau \overline{W}_i^\tau = y_i^\tau \frac{\delta_i^\tau}{T_0}\left(\frac{q_i^\tau + q_i^{\tau-1}}{2}\right) = \frac{y_i^\tau}{2T_0}\delta_i^\tau(q_i^\tau + q_i^{\tau-1}) \tag{53}$$

The convexity of $\delta_i^\tau(q_i^\tau + q_i^{\tau-1})$ is similar to the convexity of Γ''(Boyd and Vandenberghe, 2009).

$$\delta_i^\tau = T_0\chi_i^\tau + \frac{\mu_i^\tau q_i^{\tau-1}}{\mu_i^\tau - \lambda_i^\tau}(1 - \chi_i^\tau) \tag{54}$$

$$q_i^\tau = \chi_i^\tau\left(\frac{T_0}{\mu_i^n}\left(\lambda_i^\tau - \mu_i^n\right) + q_i^{\tau-1}\right) \tag{55}$$

$$\delta_i^\tau(q_i^\tau + q_i^{\tau-1}) = \left[T_0\chi_i^\tau + \frac{\mu_i^\tau q_i^{\tau-1}}{\mu_i^\tau - \lambda_i^\tau}(1 - \chi_i^\tau)\right]\left[\chi_i^\tau\left(\frac{T_0}{\mu_i^n}\left(\lambda_i^\tau - \mu_i^n\right) + q_i^{\tau-1}\right) + q_i^{\tau-1}\right] \tag{56}$$

χ_i^τ is a binary variable indicating if there is a queue in the time interval ($\chi_i^\tau = 1$) or not ($\chi_i^\tau = 0$). Therefore, the convexity of the function is evaluated for different values of χ_i^τ.

Case 1: $\chi_i^\tau = 1$

$$\Gamma^3 = \delta_i^\tau(q_i^\tau + q_i^{\tau-1}) = T_0\left(\frac{T_0}{\mu_i^\tau}\left(\lambda_i^\tau - \mu_i^\tau\right) + 2q_i^{\tau-1}\right) = \frac{{T_0}^2}{\mu_i^\tau}\left(\lambda_i^\tau - \mu_i^\tau\right) + 2T_0 q_i^{\tau-1} \tag{57}$$

(57) is convex as it is the summation of two convex terms, as proved in the above section, and this indicates the convexity of the objective function when $\chi_i^\tau = 1$.

Case 2: $\chi_i^\tau = 0$

$$\Gamma^4 = \delta_i^\tau(q_i^\tau + q_i^{\tau-1}) = \frac{\mu_i^\tau q_i^{\tau-1}}{\mu_i^\tau - \lambda_i^\tau}q_i^{\tau-1} = \frac{\mu_i^\tau(q_i^{\tau-1})^2}{\mu_i^\tau - \lambda_i^\tau} \tag{58}$$

μ_i^τ does not affect the convexity of (58). Therefore, considering $\lambda_i^\tau = \frac{y_i^\tau}{T_0 z_i}$, the convexity of this phrase can be evaluated as follows:

$$\Gamma^5 = \frac{(q_i^{\tau-1})^2}{\mu_i^\tau - \lambda_i^\tau} \tag{59}$$

$$\frac{d(\Gamma^5)}{dz} = \frac{2q_i^{\tau-1}\frac{dq_i^{\tau-1}}{dz}\left(\mu_i^\tau - \frac{y_i^\tau}{T_0 z_i}\right) - \frac{y_i^\tau}{T_0 z_i{}^2}(q_i^{\tau-1})^2}{(\mu_i^\tau - \frac{y_i^\tau}{T_0 z_i})^2} \tag{60}$$

$$\frac{d(\Gamma^5)}{dz} = \frac{2q_i^{\tau-1}\frac{dq_i^{\tau-1}}{dz}}{\mu_i^\tau - \frac{y_i^\tau}{T_0 z_i}} - \frac{\frac{y_i^\tau}{T_0 z_i{}^2}(q_i^{\tau-1})^2}{(\mu_i^\tau - \frac{y_i^\tau}{T_0 z_i})^2} \tag{61}$$

$$\frac{d^2(\Gamma^5)}{dz^2} = \frac{\left[2\left(\frac{dq_i^{\tau-1}}{dz}\right)^2 + 2q_i^{\tau-1}\frac{d^2 q_i^{\tau-1}}{dz^2}\right]\left(\mu_i^\tau - \frac{y_i^\tau}{T_0 z_i}\right) - \frac{y_i^\tau}{T_0 z_i{}^2}2q_i^{\tau-1}\frac{dq_i^{\tau-1}}{dz}}{(\mu_i^\tau - \frac{y_i^\tau}{T_0 z_i})^2} - \frac{\left[-\frac{2y_i^\tau}{T_0 z_i{}^3}(q_i^{\tau-1})^2 + 2\frac{y_i^\tau}{T_0 z_i{}^2}q_i^{\tau-1}\frac{dq_i^{\tau-1}}{dz}\right]\left(\mu_i^\tau - \frac{y_i^\tau}{T_0 z_i}\right)^2}{\left(\mu_i^\tau - \frac{y_i^\tau}{T_0 z_i}\right)^4} + \frac{2\frac{y_i^\tau}{T_0 z_i{}^2}\left(\mu_i^\tau - \frac{y_i^\tau}{T_0 z_i}\right)\frac{y_i^\tau}{T_0 z_i{}^2}(q_i^{\tau-1})^2}{(\mu_i^\tau - \frac{y_i^\tau}{T_0 z_i})^4} \tag{62}$$

As $\chi_i^\tau = 0 \rightarrow \mu_i^\tau > \lambda_i^\tau \rightarrow \mu_i^\tau > \frac{y_i^\tau}{T_0 z_i} \rightarrow \mu_i^\tau - \frac{y_i^\tau}{T_0 z_i} > 0$ Further, as proved in (48), the first derivative of q_i^τ is negative. Therefore, the second derivative is always positive since all terms in (62) are positive.

As the objective function is convex for both of the cases, we can conclude that it is always convex.

References

Andrews, M., Dogru, M.K., Hobby, J.D., Jin, Y., Tucci, G.H., 2012. Modeling and Optimization for Electric Vehicle Charging Infrastructure.

Avci, B., Girotra, K., Netessine, S., 2012. Electric vehicles with a battery switching station: Adoption and environmental impact, Management Science. https://doi.org/10.1287/mnsc.2014.1916.

Bai, Y., Hwang, T., Kang, S., Ouyang, Y., 2011. Biofuel refinery location and supply chain planning under traffic congestion. Transp. Res. Part B Methodol. 45, 162–175. https://doi.org/10.1016/J.TRB.2010.04.006.

Berman, O., Larson, R.C., Fouska, N., 1992. Optimal Location of Discretionary Service Facilities. Transp. Sci. 26, 201–211.

Boyd, S., Vandenberghe, L., 2009. Convex Optimization, seventh ed., Communication Networking. Cambridge University Press, Cambridge. https://doi.org/10.1016/B978-012428751-8/50019-7.

Cai, H., Jia, X., Chiu, A.S.F., Hu, X., Xu, M., 2014. Siting public electric vehicle charging stations in Beijing using big-data informed travel patterns of the taxi fleet. Transp. Res. Part D Transp. Environ. 33, 39–46. https://doi.org/10.1016/j.trd.2014.09.003.

Chen, T.D., Kockelman, K.M., Khan, M., 2013. Locating Electric Vehicle Charging Stations Parking-Based Assignment Method for Seattle, Washington. Transp. Res. Rec. J. Transp. Res. Board 2385, 28–36. https://doi.org/10.3141/2385-04.

Chen, R., Qian, X., Miao, L., Ukkusuri, S.V., 2020. Optimal charging facility location and capacity for electric vehicles considering route choice and charging time equilibrium. Comput. Oper. Res. 113, 104776 https://doi.org/10.1016/j.cor.2019.104776.

Dong, J., Liu, C., Lin, Z., 2014. Charging infrastructure planning for promoting battery electric vehicles: An activity-based approach using multiday travel data. Transp. Res. Part C Emerg. Technol. 38, 44–55. https://doi.org/10.1016/J.TRC.2013.11.001.

Fakhrmoosavi, F., Kavianipour, M., Shojaei, M. (Sam), Zockaie, A., Ghamami, M., Wang, J., Jackson, R., 2021. Electric vehicle charger placement optimization in michigan considering monthly traffic demand and battery performance variations. Transp. Res. Rec. J. Transp. Res. Board 036119812098195. https://doi.org/10.1177/0361198120981958.

Ghamami, M., Kavianipour, M., Zockaie, A., Hohnstadt, L.R., Ouyang, Y., 2020. Refueling infrastructure planning in intercity networks considering route choice and travel time delay for mixed fleet of electric and conventional vehicles. Transp. Res. Part C Emerg. Technol. 120, 102802 https://doi.org/10.1016/j.trc.2020.102802.

Ghamami, M., Zockaie, A., Nie, Y.M., 2016. A general corridor model for designing plug-in electric vehicle charging infrastructure to support intercity travel. Transp. Res. Part C Emerg. Technol. 68, 389–402. https://doi.org/10.1016/j.trc.2016.04.016.

Grassmann, W., 1983. The convexity of the mean queue size of the M/M/c queue with respect to the traffic. J. Appl. Probability.

Hajibabai, L., Bai, Y., Ouyang, Y., 2014. Joint optimization of freight facility location and pavement infrastructure rehabilitation under network traffic equilibrium. Transp. Res. Part B Methodol. 63, 38–52. https://doi.org/10.1016/J.TRB.2014.02.003.

He, F., Wu, D., Yin, Y., Guan, Y., 2013. Optimal deployment of public charging stations for plug-in hybrid electric vehicles. Transp. Res. Part B Methodol. 47, 87–101. https://doi.org/10.1016/J.TRB.2012.09.007.

He, J., Yang, H., Tang, T.-Q., Huang, H.-J., 2018. An optimal charging station location model with the consideration of electric vehicle's driving range. Transp. Res. Part C Emerg. Technol. 86, 641–654. https://doi.org/10.1016/J.TRC.2017.11.026.

Hodgson, M.J., 1990. A flow-capturing location-allocation. Model. Geogr. Anal. 22, 270–279. https://doi.org/10.1111/j.1538-4632.1990.tb00210.x.

Ip, A., Fong, S., Liu, E., 2010. Optimization for allocating BEV recharging stations in urban areas by using hierarchical clustering. Manag. Serv. 460–465.

Jayakrishnan, R., Mahmassani, H.S., Hu, T.-Y., 1994. An evaluation tool for advanced traffic information and management systems in urban networks. Transp. Res. Part C Emerg. Technol. 2, 129–147.

Jung, J., Chow, J.Y.J., Jayakrishnan, R., Park, J.Y., 2014. Stochastic dynamic itinerary interception refueling location problem with queue delay for electric taxi charging stations. Transp. Res. Part C Emerg. Technol. 40, 123–142. https://doi.org/10.1016/j.trc.2014.01.008.

Kavianipour, M., Fakhrmoosavi, F., Shojaei, M. (Sam), Zockaie, A., Ghamami, M., Wang, J., Jackson, R., 2021. Impacts of technology advancements on electric vehicle charging infrastructure configuration: a Michigan case study. Int. J. Sustain. Transp.

Kavianipour, M., Mozafari, H., Ghamami, M., Zockaie, A., Jackson, R., 2020. Effects of electric vehicle adoption for state-wide intercity trips on the emission saving and energy consumption.

Kavianipour, M., Saedi, R., Zockaie, A., Saberi, M., 2019. Traffic state estimation in heterogeneous networks with stochastic demand and supply: mixed Lagrangian-Eulerian approach. Transp. Res. Rec. 2673, 114–126. https://doi.org/10.1177/0361198119850472.
Kiefer, J., 1953. Sequential minimax search for a maximum. Proc. Am. Math. Soc. 4, 502. https://doi.org/10.2307/2032161.
Kim, J.G., Kuby, M., 2012. The deviation-flow refueling location model for optimizing a network of refueling stations. Int. J. Hydrogen Energy 37, 5406–5420. https://doi.org/10.1016/j.ijhydene.2011.08.108.
Krisher, T., 2019. AAA: Cold weather can cut electric car range over 40 percent [WWW Document]. URL https://apnews.com/04029bd1e0a94cd59ff9540a398c12d1 (accessed 11.4.19).
Kuby, M., Lim, S., 2007. Location of alternative-fuel stations using the flow-refueling location model and dispersion of candidate sites on arcs. Networks Spat. Econ. 7, 129–152. https://doi.org/10.1007/s11067-006-9003-6.
Kuby, M., Lim, S., 2005. The flow-refueling location problem for alternative-fuel vehicles. Socioecon. Plann. Sci. 39, 125–145. https://doi.org/10.1016/J.SEPS.2004.03.001.
Li, M., Jia, Y., Shen, Z., He, F., 2017. Improving the electrification rate of the vehicle miles traveled in Beijing: a data-driven approach. Transp. Res. Part A Policy Pract. https://doi.org/10.1016/j.tra.2017.01.005.
Lim, S., Kuby, M., 2010. Heuristic algorithms for siting alternative-fuel stations using the Flow-Refueling Location Model. Eur. J. Oper. Res. 204, 51–61. https://doi.org/10.1016/J.EJOR.2009.09.032.
MISO Energy, 2018. Real-Time Displays [WWW Document]. URL https://www.misoenergy.org/markets-and-operations/real-time-displays/ (accessed 10.15.18).
Nie, Y. (Marco), Ghamami, M., 2013. A corridor-centric approach to planning electric vehicle charging infrastructure. Transp. Res. Part B Methodol. 57, 172–190. https://doi.org/10.1016/J.TRB.2013.08.010.
Nie, Y., Ghamami, M., Zockaie, A., Xiao, F., 2016. Optimization of incentive polices for plug-in electric vehicles. Transp. Res. Part B Methodol. 84, 103–123. https://doi.org/10.1016/j.trb.2015.12.011.
Nourbakhsh, S.M., Ouyang, Y., 2010. Optimal fueling strategies for locomotive fleets in railroad networks. Transp. Res. Part B Methodol. https://doi.org/10.1016/j.trb.2010.03.003.
Riemann, R., Wang, D.Z.W., Busch, F., 2015. Optimal location of wireless charging facilities for electric vehicles: Flow capturing location model with stochastic user equilibrium. Transp. Res. Part C Emerg. Technol. https://doi.org/10.1016/j.trc.2015.06.022.
Shahraki, N., Cai, H., Turkay, M., Xu, M., 2015. Optimal locations of electric public charging stations using real world vehicle travel patterns. Transp. Res. Part D Transp. Environ. 41, 165–176. https://doi.org/10.1016/j.trd.2015.09.011.
Sheppard, G., Waraich, R., Campbell, A., Pzdnukhov, A.R., Gopal, A., 2017. Lawrence Berkeley National Laboratory Recent Work Title Modeling plug-in electric vehicle charging demand with BEAM, the framework for behavior energy autonomy mobility.
Sweda, T., Klabjan, D., 2011. An Agent-Based Decision Support System for Electric Vehicle Charging Infrastructure Deployment.
Tate, E.D., Harpster, M.O., Savagian, P.J., 2008. The electrification of the automobile: From conventional hybrid, to plug-in hybrids, to extended-range electric vehicles. SAE Tech. Pap. https://doi.org/10.4271/2008-01-0458.
Tu, W., Li, Q., Fang, Z., Shaw, S. lung, Zhou, B., Chang, X., 2016. Optimizing the locations of electric taxi charging stations: a spatial–temporal demand coverage approach. Transp. Res. Part C Emerg. Technol. 65, 172–189. https://doi.org/10.1016/j.trc.2015.10.004.
Upchurch, C., Kuby, M., Lim, S., 2009. A model for location of capacitated alternative-fuel stations. Geogr. Anal. 41, 127–148. https://doi.org/10.1111/j.1538-4632.2009.00744.x.
Usman, M., Knapen, L., Yasar, A.U.H., Bellemans, T., Janssens, D., Wets, G., 2020. Optimal recharging framework and simulation for electric vehicle fleet. Futur. Gener. Comput. Syst. 107, 745–757. https://doi.org/10.1016/j.future.2017.04.037.
Wang, C., He, F., Lin, X., Shen, Z.J.M., Li, M., 2019. Designing locations and capacities for charging stations to support intercity travel of electric vehicles: an expanded network approach. Transp. Res. Part C Emerg. Technol. 102, 210–232. https://doi.org/10.1016/j.trc.2019.03.013.
Wilaby, M., Casas, J., 2016. MI Travel Counts III.
Wood, E., Rames, C., Muratori, M., Raghavan, S., Melaina, M., 2017. National plug-in electric vehicle infrastructure analysis, NREL. https://doi.org/10.13140/RG.2.2.25881.93280.
Xi, X., Sioshansi, R., Marano, V., 2013. Simulation – optimization model for location of a public electric vehicle charging infrastructure. Transp. Res. PART D 22, 60–69. https://doi.org/10.1016/j.trd.2013.02.014.
Xie, F., Liu, C., Li, S., Lin, Z., Huang, Y., 2018. Long-term strategic planning of inter-city fast charging infrastructure for battery electric vehicles. Transp. Res. Part E Logist. Transp. Rev. 109, 261–1176. https://doi.org/10.1016/j.tre.2017.11.014.
Xie, S., Chen, X., Wang, Z., Ouyang, Y., Somani, K., Huang, J., 2016. Integrated planning for multiple types of locomotive work facilities under location, routing, and inventory considerations. INFORMS J. Appl. Anal. 46, 391. https://doi.org/10.1287/inte.2016.0857.
Yang, J., Dong, J., Hu, L., 2017. A data-driven optimization-based approach for siting and sizing of electric taxi charging stations. Transp. Res. Part C Emerg. Technol. 77, 462–477. https://doi.org/10.1016/j.trc.2017.02.014.
Zhang, K., Lu, L., Lei, C., Zhu, H., Ouyang, Y., 2018. Dynamic operations and pricing of electric unmanned aerial vehicle systems and power networks. Transp. Res. Part C 92, 472–485. https://doi.org/10.1016/j.trc.2018.05.011.
Zockaie, A., Aashtiani, H.Z., Ghamami, M., Marco Nie, Y., 2016. Solving Detour-Based Fuel Stations Location Problems. Comput. Civ. Infrastruct. Eng. 31, 132–144. https://doi.org/10.1111/mice.12170.
Zukerman, M., 2013. Introduction to Queueing Theory and Stochastic Teletraffic Models.